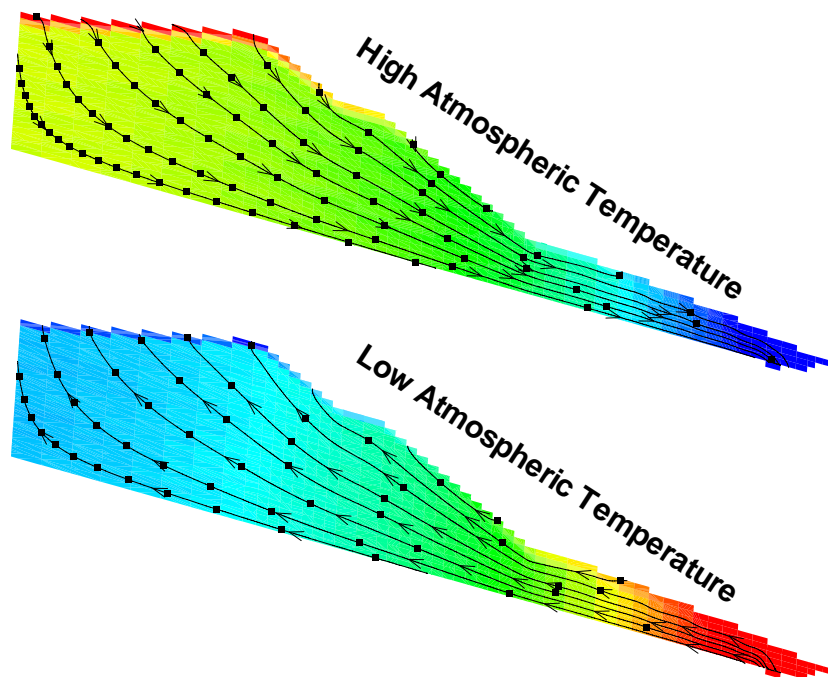


- FINAL REPORT -

Numerical Modeling of Gas Flow in the No. 1 Shaft Waste Rock Dump, Sullivan Mine, B.C., Canada

Belkacem Lahmira and René Lefebvre



Institut national de la recherche scientifique
Centre Eau Terre Environnement

Research Report R-970

July 2008



- FINAL REPORT -

Numerical Modeling of Gas Flow in the No. 1 Shaft
Waste Rock Dump, Sullivan Mine, B.C., Canada

Belkacem Lahmira and René Lefebvre

Institut national de la recherche scientifique, Centre Eau Terre Environnement

Research carried out under contract with
Teck Cominco Limited

Report submitted to
Mr. Walter J. Kuit, Director, Environmental Science
Teck Cominco Limited, Vancouver, Canada

Institut national de la recherche scientifique
Centre Eau Terre Environnement

Research Report R-970

July 2008

Executive Summary

The Sullivan Mine No. 1 Shaft Waste Rock Dump is located on a natural slope and covered by till. The outflow of oxygen-deprived gas through a leachate drainage pipe in an enclosure at the base of the dump resulted in four fatalities. Our mandate was to develop a numerical model to test the plausibility of physical mechanisms that were hypothesized to be controlling gas flow.

The numerical model confirms that gas flow is controlled by atmospheric temperature. Gas comes out of the drainage pipe when atmospheric temperature is higher than an equilibrium value. On the other hand, air enters the pipe when atmospheric temperature is lower than the equilibrium value. The value at which there is no gas flow is equivalent to the average internal dump temperature. Steady state flow conditions are rapidly reached, in 15-20 minutes, even after the major simulated initial perturbation in atmospheric temperature and pressure. Since the system rapidly responds, pipe flow rates can closely follow atmospheric temperature changes.

Gas flow is controlled by the relative buoyancy of the dump gas phase compared to atmospheric air, which is related to their relative densities. Barometric pressure has an insignificant effect on gas flow, as it barely modifies the relative densities of dump gas and atmospheric air. The presence of CO₂ in the dump gas phase makes its molar mass equivalent to the one of atmospheric air. This implies that dump gas composition does not either influence the relative densities of dump gas and atmospheric air. Changes in atmospheric air density are caused by atmospheric temperature variations, whereas the dump gas phase density is nearly fixed by the steady internal dump temperature. When atmospheric temperature is lower than the internal dump temperature, atmospheric air density is higher than dump gas density, inducing upward dump gas flow and air entry in the pipe. Instead, downward dump gas flow occurs and exits the pipe when high atmospheric temperature leads to an air density lower than dump gas density.

Gas flow is facilitated by a coarse fill material that was placed in a ditch along the dump toe prior to covering of the pile. The coarse material focuses outward gas flow towards the pipe, and distributes inward gas flow from the pipe along the toe of the waste. Effective air permeabilities of waste rock and till cover significantly higher than initial estimates had to be used to exactly match observed pipe gas velocities. This could reflect the combined effects of coarse preferential flow paths in waste rock and localized variability in the cover. The relatively low permeability of the till cover still significantly limits gas exchanges between the dump and atmosphere. However, a very low permeability till cover is not required to get gas flow as observed at the site. On the contrary, a perfectly sealing dump cover would lead to a very different gas flow behavior. The model also shows that, under the conditions found in the No. 1 Shaft Dump, similar gas flow patterns would prevail without the pipe or without the till cover. The magnitude of gas flow would change though, gas flow being reduced without a pipe but enhanced without a cover.

The No. 1 Shaft Dump is probably typical of some other covered dumps, which generally have steadily decreasing internal temperature and an oxygen-deprived gas phase, and where CO₂ can be generated if carbonates are present in the waste rock. Such conditions in other covered dumps could lead to gas flow behavior similar to what is observed at the No. 1 Shaft Dump. This gas flow behavior could potentially be found also in uncovered dumps having a mean internal temperature within the yearly range of variation of local atmospheric temperature.

Table of Content

<u>1. INTRODUCTION</u>	<u>1</u>
<u>2. NUMERICAL MODEL DEVELOPMENT</u>	<u>3</u>
2.1 MONITORING DATA REVIEW	3
2.2 SIMPLIFYING ASSUMPTIONS	6
2.3 MODEL DISCRETIZATION	8
2.4 MATERIALS AND CONDITIONS	9
<u>3. NUMERICAL MODELING RESULTS</u>	<u>15</u>
3.1 TEMPERATURE CONTROL ON GAS FLOW	16
3.1.1 HYDROSTATIC CONDITIONS	16
3.1.2 STEADY STATE GAS FLOW IN THE DUMP	16
3.1.3 STEADY STATE GAS FLOW IN THE PIPE	17
3.2 BAROMETRIC PRESSURE EFFECT ON STEADY STATE FLOW	18
3.3 TRANSIENT GAS FLOW CONDITIONS	19
3.4 GAS FLOW WITHOUT A TILL COVER	19
3.5 GAS FLOW WITHOUT A PIPE	20
<u>4. DISCUSSION ON PROCESSES CONTROLLING GAS FLOW</u>	<u>23</u>
4.1 PNEUMATIC POTENTIAL CONTROLLING GAS FLOW	23
4.2 GAS FLOW CONCEPTUAL MODEL	29
<u>5. CONCLUSIONS</u>	<u>33</u>
<u>6. REFERENCES</u>	<u>37</u>

Tables, Figures and Appendix

(Tables, figures and appendix are found at the end of the report)

Tables

Table 1. Estimated gas densities in monitoring boreholes compared to atmospheric air densities	41
Table 2. Temperature and pressure conditions with corresponding pneumatic potential.....	42
Table 3. Material properties.....	43
Table 4. Simulated gas velocities (m/d) in the waste rock dump	44
Table 5. Simulated gas densities and velocities through the pipe.....	45
Table 6. Simulated pipe gas velocities related to changes in barometric pressure at 36 °C	45
Table 7. Steady state pipe gas flow velocities without a till cover	45
Table 8. Summary of monitored conditions in boreholes.....	46

Figures

Figure 1. Location of Section 0+525 used to develop the numerical grid.....	49
Figure 2. Selected monthly temperature profiles in boreholes	50
Figure 3. Second order polynomial fit to mean temperatures in boreholes BH-1A and BH-1B..	51
Figure 4. Projection of boreholes on the numerical grid section	52
Figure 5. Boundary conditions and materials distribution in the numerical grid	52
Figure 6. Simulated conditions for low (top) and high (bottom) atmospheric temperature	53
Figure 7. Comparison of simulated and measured gas velocities in the pipe	54
Figure 8. Correlation between normalized temperatures and pipe gas velocities.....	54
Figure 9. Transient pipe gas velocities for various atmospheric temperatures (top) and pressures at 36 °C (bottom).....	55
Figure 10. Transient gas mass in the dump for various atmospheric temperatures (top) and pressures at 36 °C (bottom).....	56
Figure 11. Simulated conditions at 5 °C without a till cover (bottom) compared to conditions with a dry till cover (top)	57

Figure 12. Simulated conditions without a pipe for a dry till cover at 5 °C (top) and 36 °C (bottom).....	58
Figure 13. Pneumatic potential and streamtraces at 5 °C for the dry till cover with the pipe (top), without a pipe (middle) and with a pipe but without a till cover (bottom).....	59
Figure 14. Pneumatic potential and streamtraces at 36 °C for the dry till cover with the pipe (top), without a pipe (middle) and with a pipe but without a till cover (bottom).....	60
Figure 15. Vertical distribution of pneumatic potentials at 5 °C (left) and 36 °C (right) for the dry till cover with the pipe (top), without a pipe (middle) and without a till cover (bottom).....	61
Figure 16. Comparison of the conceptual model of gas flow with numerical results for low (top) and high (bottom) atmospheric temperatures	62

Appendix

Appendix 1: Complementary simulation results and figures	65
Appendix 2: Compilation of Gas Flux, Velocity and Mass.....	77
Appendix 3: Estimation of material properties.....	87

1. Introduction

This report documents the results of a research project carried out by INRS under a contract with Teck Cominco Limited titled “Development of a numerical model to provide a representation of physically-plausible mechanisms that could be controlling gas flow in the Sullivan Mine No. 1 Waste Dump”. A fatal accident occurred at the No. 1 Shaft Waste Dump of the Sullivan Mine, B.C. This accident is thought to be related to the downward flow of oxygen-deprived air originating from the waste dump. That air is presumed to have entered a water sampling enclosure located at the base of the waste dump through the water sampling pipe.

The objective of the project was to develop a numerical model to test the plausibility of various physical mechanisms that were hypothesized to be controlling gas flow in the Sullivan Mine No. 1 Shaft Waste Dump. The numerical simulator used was TOUGH AMD, which can represent physical processes related to AMD production in waste rock (Lefebvre, 1995; Lefebvre and G elinas, 1995; Lefebvre et al., 1998, 2001b, 2001c, 2002; Smolensky et al., 1999; Wels et al., 2003; Sracek et al., 2004). Simulations used simplifying assumptions described in the next section, while keeping the model representative of conditions found at the site. A series of simulations were carried out to cover the range of material properties and conditions found at the site. Reports and data made available were reviewed and used to estimate material properties (Phillip and Hockley, 2007; Kimberley Incident Technical Panel, 2007). A review of available monitoring data was also made to develop a representative conceptual model of gas flow at the site that formed the basis for numerical modeling (personal communication of R. Lefebvre to D. Hockley, Dec. 2007). The validation and calibration of the model was achieved by the modeling of monitored conditions that were “reproduced” by the model. The key model parameters (air permeability of waste and cover) were adjusted to better represent the general gas flow behavior monitored at the exit pipe (and in a more general way within the dump).

The present scope of work is limited to the understanding of the No. 1 Shaft Waste Dump and does not include simulations that would aim to define the general conditions under which gas flow could represent a safety hazard at other waste rock dump sites.

2. Numerical Model Development

2.1 *Monitoring Data Review*

Figure 1 shows the location of monitoring boreholes and other monitoring facilities that were available when the numerical model was developed. The available data were reviewed to estimate material properties and develop a conceptual model of gas flow that was used as a basis for the numerical model development. The estimation of initial material properties is described in Section 2.4 and documented in Appendix C. This section briefly describes the temperature and gas composition data that were assessed in order to define representative model conditions. The conceptual model is described in Chapter 4, which discusses the processes controlling gas flow.

Figure 2 shows selected monthly temperature profiles measured in monitoring boreholes. Except for BH-1A and BH-1B, boreholes are shallow and temperatures are measured in the zone affected by cyclic yearly atmospheric temperature variations, which appears to be about 8 m deep in the waste rock dump. A sinusoidal fit to monitored atmospheric temperature showed that it could be represented by a mean surface temperature of 7.5 °C and a total annual change in temperature of 31 °C (not shown). For boreholes BH-1A and BH-1B, there are sufficient temperature measurements beyond the zone affected by cyclic surface temperature changes to determine a mean temperature profile using the available data (Figure 3). Average values of temperature were calculated at each measuring depth using the selected monthly profiles shown on the Figure 2. Data points obtained for both boreholes were combined in Figure 3 and a good regression could be made to the data with a second order polynomial.

Temperatures observed in the dump are very similar for BH-1A and BH-1B and clearly higher than the atmospheric mean value of 7.5 °C. This implies that similar internal heat production occurs related to sulfide oxidation at these two locations. Furthermore, the relatively steady curvature of the temperature profile shown on Figure 3 could be indicative of heat production over the entire thickness of the pile. Similarly shaped temperature profiles observed at a Questa Mine, New Mexico, waste rock dump were shown to be related to lateral gas flow that could bring oxygen over the entire thickness of the dump (Lefebvre et al., 2002; Wels et al., 2003). However, the relatively low temperatures are indicative of moderate heat production that could

be related to limited gas flow and oxygen supply available to support sulfide oxidation. Caution must be used in the interpretation of temperature data as they may partly represent residual heat remaining to be dissipated following the placement of the till cover on the dump.

The observed thermal conditions in the No. 1 Shaft Dump show that temperatures are similar at central locations in the dump and remain quite stable throughout the year. This is an important observation as it was used to make the simplifying assumption that internal dump temperature could be fixed in the numerical model. These temperature profiles could also serve as baseline to be compared to long-term measurements of temperature in the dump. This comparison could provide a global indication of the effectiveness of the till cover. If the cover is effective, it should limit air inflow and oxygen supply, thus also limit heat production, such that temperature should be steadily decreasing in the dump. In the case of the No. 1 Shaft Dump, such interpretation will have to take into account the important gas exchanges occurring through the drain pipe. The pipe allows bypassing of the till cover at the base of the dump, which likely reduces the apparent performance of the cover in limiting gas exchanges between the dump and the atmosphere.

Another condition assessed on the basis of the monitoring data is the composition of dump gas. Gas composition was determined on dump gas flowing out of the drain pipe as well as in gas sampled from ports installed in monitoring boreholes. Equation 1, presented in Section 4.1, indicates that gas density is determined by its pressure, temperature and molar mass. The molar mass being itself fixed by the molar fractions and masses of the components present in the gas phase. In ARD-producing waste rock dumps, oxygen consumption would generally lead to a lower molar mass for the gas phase, as its own molar mass (32 g/mol) is higher than the mean dry atmospheric air molar mass (29 g/mol), which is controlled by the nitrogen molar mass (28 g/mol). This reduction of the waste rock dump gas molar mass is further accentuated by the increase in water vapor content (molar mass of 18 g/mol) if the internal dump temperature is high, which increases water vapor partial pressure and its proportion of the dump gas phase. In the No. 1 Shaft Dump, there is a relatively high proportion of CO₂, which has a high molar mass (44 g/mol). Dump gas outflow at the pipe can have more than 5 or 6% CO₂, whereas concentrations between about 2 and 6% were measured in boreholes (Table 1).

In waste rock dumps where temperatures are high, the reduction in density due to these temperatures is such that strong upward thermal gas convection occurs, as shown at Mine Doyon where values exceeding 60 °C were observed (Lefebvre and G elinas, 1995). The lightening of the gas phase caused by oxygen depletion can also lead to upward gas convection in dumps with lower internal temperatures, as demonstrated for the Nordhalde in Germany where internal dump temperatures were mostly lower than 16 °C (Lefebvre et al., 1998; Smolensky et al., 1999). The moderate internal dump temperatures between 10 and 15 °C observed in the No. 1 Shaft Dump and the high concentrations in CO₂ in the dump gas could potentially lead to molar masses and densities similar to atmospheric air. This could lead to reversals in the vertical flow tendency of dump gas relative to atmospheric air.

Table 1 shows results of calculations made to assess the effects of CO₂ concentrations, internal dump temperatures and atmospheric temperatures on the relative densities of dump gas and atmospheric air. Calculations were carried out for representative gas concentrations observed in boreholes. The presence of water vapor and relative humidity were considered. The first result of interest is the very similar humid gas molar mass for atmospheric air and dump gas for all boreholes. This implies that when atmospheric air has the same temperature as the dump, its density would be identical to dump gas density. Relative density is defined here as the ratio of borehole gas density over atmospheric air density. Buoyancy should make the dump gas tend to flow up when the relative density is lower than unity. Relative densities were calculated for a range of observed atmospheric temperatures (Low, Mean and High). On the basis of its relative density, Table 1 shows that dump gas should tend to flow upward when atmospheric temperature is low and downward when it is high. This is coherent with observed pipe gas flow directions as a function of atmospheric temperature. The relative density of dump gas and atmospheric air can thus be considered a potential driving mechanism for gas flow in the No. 1 Shaft Dump. These results further indicate that dump gas molar mass can be considered similar to atmospheric air, and this throughout the entire dump as all boreholes showed similar general gas flow tendencies. This supports the simplifying assumption that gas composition changes do not have to be considered in the numerical model. These results also indicate that dump gas composition, especially the presence of CO₂, has to be taken into account while assessing potential dump gas flow directions in low temperature dumps.

2.2 Simplifying Assumptions

The number of unknowns needed to specify the state of a numerical system depends on the number of phases and components considered (Pruess et al., 1999). Waste rock dumps in which acid mine drainage (AMD) is occurring are partially water saturated media within which oxygen consumption occurs due to sulfide oxidation (mostly pyrite), which leads to heat production (Lefebvre et al., 2001a). Numerical simulation of AMD in waste rock dumps thus involves the simultaneous estimation of four unknowns to determine the state of the system (gas pressure, water saturation, mass fraction of oxygen and temperature). The simulator also has to calculate the equation of state defining the equilibrium concentration of components (water, air and oxygen) in the two fluid phases (gas and liquid) as a function of temperature. This numerical problem is thus demanding, so that detailed numerical grids would require a long computation time to solve for the transient evolution of the system. For the numerical simulation of AMD production in waste rock, it is thus normally preferred to use relatively coarse grid elements, while capturing the most important features of the dump geometry and material distribution (Lefebvre et al., 2001b).

Compared to the general case of AMD in waste rock, specific conditions prevailing in the No. 1 Shaft Dump at the Sullivan Mine allow the modeled system to be simplified as follows:

- **Thermal conditions.** Isothermal (fixed temperature) conditions can be used with different temperatures assigned to the dump and atmosphere, but without considering heat transfer, thus avoiding the need to solve for temperature;
- **Gas composition.** Fixed gas composition, equivalent to atmospheric air, assigned to gas phases in the dump and atmosphere, thus avoiding the need to solve for gas composition;
- **Water flow.** Fixed water saturations, at different values for waste rock and till cover, imposed as residual water. This implies that no liquid water flow is represented, thus avoiding the solution of highly non-linear liquid flow under unsaturated conditions.

Isothermal conditions can be used since it was shown that the average temperature in the dump is relatively uniform and remains relatively constant throughout the year below a certain depth (Figures 2 and 3). Internal dump temperature is thus relatively independent of atmospheric

conditions. Different simulations were thus carried out with a fixed temperature assigned to waste rock but at different values of atmospheric temperature in contact with the dump surface. However, since the simulator cannot represent temperatures lower than 0 °C, involving water freezing, mean dump temperature was shifted upward in numerical simulations as well as the atmospheric temperatures representing the range of variations observed at the site.

Fixed gas composition can be imposed in the numerical model because the dump gas phase was shown to have a mean molar mass similar to atmospheric air (Table 1). Although the dump gas phase is depleted in oxygen, which would lower the molar mass, it contains a proportion of CO₂ that brings its molar mass close to atmospheric air (Table 1). Under such conditions, the dump gas phase composition will not significantly influence its density relative to atmospheric air. Using the same equivalent composition for both gas phases should thus lead to representative gas flow. This simplifying assumption avoids the need to represent oxygen consumption related to AMD production due to sulfide oxidation.

The dump is a partially water saturated media in which there is slow water infiltration, first through the till cover and then the underlying waste rock. However, the presence of the low permeability till cover spreads water flow relatively evenly throughout the year; even though it may vary seasonally, being expected to be higher during and following spring snow melt. Such conditions result in relatively stable water saturations whose influence on gas flow should remain quite constant throughout the year. Thus, including the solution of water flow in the system would not enhance the representation of gas flow. In order to impose water saturations representative of the system in the till cover and waste rock, while keeping water immobile, residual water saturation values were increased in the numerical model above imposed water saturations for each material. Under these conditions, the permeabilities of materials used as input in the numerical model correspond to effective air permeabilities controlling gas flow. Still, to take into account the effect of varying water saturations in the till cover, two simulation scenarios were used to represent “wet” and “dry” water saturation in the till cover and their corresponding effective permeabilities.

2.3 Model Discretization

Numerical modeling of gas flow related to AMD production in waste rock dumps is almost always carried out on two-dimensional vertical sections (Lefebvre et al., 2001b). Such models allow the representation of gas convection due to composition or temperature changes in the dump. Such convection has a strong vertical component, thus requiring the representation of vertical gas movements, but is most times not significantly changing laterally, thus not needing 3D models. Figure 1 shows the location of Section 0+525, which was used as a basis for the 2D vertical numerical grid of the No. 1 Shaft Waste Dump. This section was selected because it is representative of the central part of the dump and is surrounded by monitoring boreholes and the weather station. Since the dump has a wide central part, gas flow should predominantly be from the wide slope to the top surface and could thus be approximated as two-dimensional. A 2D vertical section numerical model having a similar width as the dump should thus be representative of the bulk gas flow in the dump.

Figure 4 shows the projected locations of boreholes on Section 0+525. Together, Figures 4 and 5 summarize the main features of the numerical grid and the distribution of materials. The grid represents the slopes at the surface of the dump as well as its base, which is inclined 8° relative to the horizontal. With TOUGH AMD, the numerical solution is independent of absolute coordinates and the geometry shown on Figure 5 was obtained by rotation and translation of the numerical grid for plotting purposes. All grid elements are vertically 1 m thick, but their lengths range from 2.5 to 10.0 m to allow a better representation of the different slopes. The horizontal transverse width of grid elements is 350 m in order to obtain a numerical model with a volume equivalent to the No. 1 Shaft Dump. The grid has a total of 889 elements, of which 53 are non active and serve to impose atmospheric conditions at the dump surface, and 1 element is non active to impose atmospheric conditions at the pipe located within toe drain fill material at the outside base of the dump. This pipe is where gas velocity, temperature and composition are monitored as gas flows in or out of the pipe. The area of the non active element representing the pipe in contact with an active drain element was assigned a value of 0.1257 m^2 , which represents the actual flow area of the pipe. This area should lead to representative simulated gas fluxes through the pipe.

2.4 Materials and Conditions

Figure 5 shows the distribution of materials and boundary conditions assigned to the numerical grid. At the surface of the dump, two single layers of 1 m thick elements are used to respectively represent non active (fixed) boundary conditions and the underlying till cover. Almost all the dump interior is assigned to waste rock material, except the high permeability fill material in the toe drain at the outer base of the dump. The pipe used to sample leachate and through which gas flows is within that drain material and it is a non active element to which atmospheric conditions are assigned. The inside limit and base of the dump are supposed impermeable and thus specified as no flux boundaries. Surface non active elements are assigned atmospheric temperature and pressure conditions. These non active elements are specified as having the same properties as waste rock in order not to artificially increase the thickness of low permeability till cover elements. Atmospheric temperature is uniformly assigned to non active boundary elements, including the dump surface and pipe. However, atmospheric pressure has to be applied with a value decreasing with elevation in accordance to the atmospheric air density in order to represent a stagnant hydrostatic gas column. Otherwise, the applied pressure could induce gas flow in the dump. Even though non active surface elements are assigned an atmospheric temperature different from the internal dump temperature, no heat transfer is considered. However, imposing atmospheric temperatures to non active surface elements provides inflowing air densities and viscosities representative of atmospheric temperature.

Monitoring data from the weather station show that temperature varies by about 30 °C, from -8 to 23 °C, and barometric pressure ranges from 85 000 to 88 000 Pa, with a mean of about 86 700 Pa (raw uncorrected pressures at the elevation of the weather station located on the dump). Monitoring data also show no gas flow through the pipe, so no gas exchange between the dump and atmosphere, when atmospheric temperature is around 10 to 12 °C. This “equilibrium” temperature thus represents the effective mean global gas temperature in the dump, considering that the dump gas phase has a molar mass equivalent to atmospheric air (Table 1). The magnitude of gas exchanges between the dump and atmosphere depends on the departure of atmospheric temperature from the equilibrium temperature. In order to simulate these gas exchanges, the numerical model thus has to represent the full range of 30 °C temperature

variations. However, the equation of state in TOUGH AMD cannot represent temperatures under 0 °C. Despite this limitation, since it is the departure in temperature relative to the equilibrium that controls gas exchanges, the model uses an equilibrium temperature of 25 °C, which allows the model to represent ± 15 °C changes without reaching negative values.

Table 2 summarizes the range of atmospheric temperatures and corresponding atmospheric pressures imposed as boundary conditions based on observed variations at the site. Base simulations at hydrostatic conditions, without gas flow in the dump, are carried out at 25 °C, the model temperature assigned to the dump. These simulations provide the initial conditions used for simulations carried out at other temperatures. The report highlights results obtained for the two “extreme” temperature cases at 5 and 36 °C representing the normal range of variation for atmospheric temperature at the site. Intermediate simulations were carried out every 5 °C between 5 and 45 °C to obtain a complete view of simulated conditions and verify if the gas flow behavior was “linear” between the two extreme values (results shown in Appendix 1). Table 2 also shows the atmospheric pressures corresponding to imposed atmospheric temperatures. These different atmospheric pressures strictly depend on the changes in temperature that induce different gas densities, thus leading to significant changes in barometric pressure due to the high elevation of the site. Table 2 shows pressure values imposed at the top of the dump and at the pipe located near its base. The barometric pressure imposed on the dump surface varies about linearly with elevation between these two values.

Table 3 summarizes the material properties derived from available data on the No. 1 Shaft Waste Rock Dump. Appendix C provides details on the estimation of these properties. Till properties were determined on the basis of available laboratory and field measurements. Using available grain size distributions, waste rock properties were estimated by comparison of its grains size distribution to analog waste rock whose properties were measured in the lab. Representative soil moistures of the till for wet and dry conditions were based on measured soil moisture profiles on the No. 1 Shaft Dump. A representative waste rock soil moisture was obtained by assuming capillary equilibrium with the till cover. Estimated capillary properties and relative permeability functions of till and waste rock are illustrated in Appendix C.

Material properties were modified from their initial estimate to calibrate and validate the model. The following criteria were used to determine if the model was representative and appropriately calibrated: 1) the direction (in or out) and magnitude of pipe gas flow as a function of atmospheric temperature; 2) the gas pressure gradients generated between the dump and atmosphere as compared to those measured at observation wells; 3) the gas flow patterns as compared to inferred patterns based on gas pressure gradients and gas composition measured in observation wells; and 4) the time for the system to reach steady state, as monitoring data show that pipe gas velocities and directions quickly follow changes in atmospheric temperature with a short lag time. Table 8 summarizes the main observations made by the No. 1 Shaft Dump monitoring system that form the basis of the model calibration criteria. These conditions and their inferred implications on gas flow are discussed in Section 4.2 on the conceptual model.

The effective air permeability is the property that had to be modified the most to calibrate the model. The value of effective air permeability had to be significantly increased, to at least $5 \times 10^{-12} \text{ m}^2$ for the till cover and $5 \times 10^{-9} \text{ m}^2$ for waste rock, in order to reproduce the observed gas flow behavior of the dump, especially the magnitude of pipe gas flow velocity. These values represent increases of more than 1 and 2 orders of magnitude, respectively, for the dry and wet till cover. For waste rock, the increase in effective air permeability over the initial estimate is 2 orders of magnitude. Such large increases above estimated values for the till cover, especially under wet conditions, were thought to indicate that the threshold effective air permeability required to calibrate the model is more likely related to local variability in the cover (fissures, grain size variations, compaction or thickness variations, etc.), than a poor initial estimate of the properties of “sound” till cover. The presence of such local variability is perhaps indicated by the observed localized melting of snow over the dump surface that could be due to preferential warm gas exit from the dump. Similarly, the large increase in effective air permeability for the waste rock over the initial estimate could reflect the heterogeneity of the dump and the presence of preferential gas flow paths through coarse high permeability material. The variability in the waste rock grain size appears to be confirmed by the recent geophysical and drilling investigations. Lahmira et al. (2007) have shown through numerical simulations that heterogeneous waste rock leads to water flow through fine-grained material, leaving coarse permeable material available for gas flow.

It is important to point out that simulations used “equivalent” homogeneous material properties to represent the till cover and waste rock that are likely heterogeneous. These equivalent properties departing from initially estimated properties do not imply that these initial estimates were necessarily wrong or that the cover is generally performing more poorly than what lab and field measurements would tend to show. Instead, these equivalent properties are thought to be strongly influenced by the presence of preferential flow paths in waste rock and local variability of the till cover. Furthermore, properties of waste rock and till cover are not independent and other combinations of these properties could as well have led to model calibration. The presence of preferential gas flow paths through the waste could also have an effect on the equivalent cover permeability. The preferential flow paths would allow high pneumatic potential gas to be in contact with localized points of the cover. If some of those points were more permeable than the bulk of the cover, significant gas flow could result. When the model is calibrated by adjusting the equivalent homogeneous bulk properties of the waste rock and cover, these localized effects cannot be considered. The implication of this discussion is that the calibration of the till cover permeability should not be taken to represent a “correction” to the original estimates.

The most important evidence supporting the use of high equivalent air permeabilities for the till cover and waste rock is provided by the observed gas flow behavior of the dump itself. If the till cover were “perfectly” impermeable, the gas flow behavior would be quite different. Pressure equilibration between dump gas and the atmosphere would occur by gas circulation through the pipe. However, there would be zero gas flow under steady state after pressure equilibration. Since, on the contrary, it is gas buoyancy that is found to control gas flow, this process requires that “significant” gas flow takes place through the till cover, which supports the required increase in air permeabilities to calibrate the model. As will be discussed in Section 4, the observation that temperature controls pipe gas velocity is a clear indication that the mechanism of gas buoyancy is controlling gas flow in the No. 1 Shaft Dump.

Under the assumption that the effective air permeability required to calibrate the model did not reflect intact till cover but the potential effect of preferential paths through the cover, the same effective air permeability was used for both dry and wet till. If local variability controls the overall cover permeability, it would not be of interest to investigate values even higher than the

“threshold” required for calibrating the model. Under such conditions, this report presents no discussion of differences between dry and wet till simulations, as these lead to very similar results. The different porosity of wet and dry cover has an effect on gas velocity through the cover but not on gas mass fluxes.

3. Numerical Modeling Results

Gas flow can be generated by gradients in gas pressure, temperature or composition (Lefebvre, 2006). All these mechanisms can potentially contribute to gas flow in a waste rock dump. Heat production related to sulfide oxidation can increase temperature and lead to thermal gas convection (Lefebvre et al., 2001b). Barometric pressure changes can also generate pressure gradients between the gas present in a dump and the atmosphere and cause gas transfer with the atmosphere by compression or expansion of the dump gas column (Wels et al., 2003). Chemical reactions in dumps can consume oxygen related to sulfide oxidation and release CO₂ by carbonate dissolution, which can alter the molar mass and density of the dump gas phase, leading to gas flow related to positive or negative dump gas buoyancy relative to atmospheric air. Furthermore, these three gas flow processes are not independent as, for example, gas temperature or composition changes can alter gas pressure.

For the numerical simulation of gas flow in the No. 1 Shaft Waste Rock Dump, different emphasis was placed on the representation of the three potential gas flow processes. As explained before, gas flow related to gas composition changes was neglected *a priori* based on available data showing that dump gas molar mass is equivalent to the one of atmospheric air (Sections 2.1 and 2.2; Table 1). Special emphasis was placed on the representation of the effect of atmospheric temperature on dump gas flow, since pipe gas velocity monitored at the site was observed to be strongly correlated to atmospheric temperature. A systematic set of simulations were run every 5 °C at temperatures below and above the equilibrium temperature fixed at 25 °C for the purposes of numerical modeling. These simulations were made twice using the properties of dry and wet till cover. In this report, the emphasis is placed on the description of results for the minimum and maximum atmospheric temperatures of 5 and 36 °C, respectively. Only the dry till cover case is discussed because, after the calibration process discussed in the preceding section, the dry and wet till cover cases produced very similar results. Complementary simulations were also carried out to investigate 1) the effect of high and low barometric pressures at 36 °C for the dry till, 2) what would happen if there were no pipe, and 3) the impact of not having a till cover on the dump, in the last two cases at 5 and 36 °C for dry and wet till.

3.1 Temperature Control on Gas Flow

3.1.1 Hydrostatic Conditions

Atmospheric pressure conditions are imposed on the numerical grid on the non active elements representing the surface of the dump and on the pipe, which is in contact with the atmosphere. The atmospheric gas column is itself static and at the simulation equilibrium temperature of 25 °C, the dump gas column also has to be static. Simulated static conditions at 25 °C are used as initial conditions for other simulations. Since gas flow is very sensitive to minute changes in pressure, it is necessary to carry out preliminary simulations at every temperature to be used later in order to define the hydrostatic pressure profile that will be used as boundary atmospheric conditions. These hydrostatic conditions are obtained by imposing pressure on a single non active element at the dump surface and then letting pressures equilibrate until there is no gas flow under steady state conditions. The pressures obtained for the boundary elements were then assigned to these elements that are made non active in subsequent simulations. Figures of these simulations are presented in Appendix 1 to show that insignificant gas flow was achieved and that boundary conditions used in the simulation do not artificially induce gas flow.

3.1.2 Steady State Gas Flow in the Dump

The effect of variations in atmospheric temperature on gas flow in the dump was studied by applying temperatures ranging from 5 to 45 °C and related barometric pressures on non active boundary elements at the surface of the dump and on the pipe. Dump temperature was maintained at 25 °C and the initial dump gas pressures corresponded to hydrostatic conditions at 25 °C. Due to such initial conditions, the onset of these simulations thus represents a sudden change in boundary temperatures and pressures, which induces transient dump gas flow conditions until the dump gas pressure distribution has equilibrated with imposed conditions. As these equilibrium conditions are reached, steady state dump gas flow related to imposed conditions is reached and pressure or gas flow patterns remain constant. These steady state flow conditions are the ones presented in this section. Figure 6 shows simulated gas flow for the base case conditions at 5 and 36 °C with a dry till cover. Arrows represent gas velocity vectors whose dimensions are proportional to velocity and gas pressure is presented with a color scale.

At the low atmospheric temperature of 5 °C, gas flow is generally from the base to the top of the dump (upper graph, Figure 6). Most gas enters through the pipe and toe drain at the base of the dump and exits through the top surface of the dump. In the lower part of the dump there is some gas entering through the till cover over at the dump surface, whereas some gas exits through the upper part of the dump slope. Gas velocities are highest in the thin lower part of the dump and velocities are progressively reduced as gas enters in the thicker internal portions of the dump.

The lower graph of Figure 6 shows gas flow conditions at the high atmospheric temperature of 36 °C. Under such conditions, gas flow is generally from the top to the base of the dump. There is limited gas exchange through the till cover over the dump slope, inward in the upper portion of the slope and outward in the lower part. As for the previous case, gas velocities are low in the thick upper portion of the dump and highest in its thin lower part. Gas flow patterns are overall similar, but in reverse direction, for the 5 and 36 °C conditions, but the magnitude of gas flow is lower at 36 °C than at 5 °C.

The steady state dump gas flow conditions illustrated in Figure 6 are fixed for the atmospheric temperatures used. In the actual system of the No. 1 Shaft Dump, atmospheric conditions are continuously changing. So gas flow in the dump varies in magnitude and directions between the conditions illustrated at 5 and 36 °C, which is a representative range of temperature change above and below the equilibrium temperature of 25 °C used in simulations.

3.1.3 Steady State Gas Flow in the Pipe

Figure 7 compares measured pipe gas velocities as a function of atmospheric temperature to numerical simulation results. Pipe gas velocities provide the best indication of the importance and direction of gas flow in the dump. At the equilibrium temperature of 10-12 °C, there is no gas flow through the pipe, whereas pipe gas velocity is positive (into the pipe) at temperatures lower than the equilibrium and negative (out of the pipe) at temperatures above the equilibrium. Pipe gas velocity is strongly negatively correlated to atmospheric temperature ($R^2=0.934$). Simulated pipe gas velocities very closely reproduce observations, showing that the model is properly calibrated. The model is also validated by comparison to other monitoring observations that are coherent with simulation results (next chapter). Table 5 compiles the pipe gas velocities

obtained at simulations carried out at various atmospheric temperatures and shows the 13 °C lower actual site temperatures corresponding to the values used in simulations. Due to the use of the same effective air permeabilities of materials, simulations with dry or wet till cover have almost identical pipe gas velocities.

Observed velocities on Figure 7 tend to be higher (positively or negatively) than the regression line and simulated results. Perhaps this could be due to the fact that simulations represent steady state gas flow conditions, whereas the actual system is always dynamically adapting to varying atmospheric conditions, which involve higher velocities (next section). Figure 8 shows that there is a short time lag of 1 to 3 hours between reductions in temperature and increases in pipe gas velocities. The lag for decreasing velocities (increasing temperatures) is almost absent. Such a time lag would appear on Figure 7 as pipe gas velocities higher than the regression or steady state simulation results. However, some peak variations in atmospheric temperature are not followed by correspondingly as high measured pipe gas velocities, which would correspond to some of the observed velocities being lower than the regression or simulation prediction.

3.2 Barometric Pressure Effect on Steady State Flow

In order to evaluate the effect of barometric pressure changes on dump gas flow, simulations were carried out with increased and decreased barometric pressures (± 2 kPa) compared to the base case for the high atmospheric temperature of 36 °C, for dry and wet till covers. New hydrostatic pressure profiles were first simulated at the equilibrium temperature of 25 °C for these modified barometric pressures in order to impose appropriate boundary conditions. Compared to the base case, there is a very slight (2%) increase in steady state gas velocities at higher barometric pressure, whereas velocities are barely decreased at lower barometric pressure (Table 4b). Table 5 shows that changes in steady state pipe gas velocities are quite insignificant under different barometric conditions. Otherwise, dump gas flow patterns at different barometric pressures are almost identical to those obtained for the base case. For this reason, figures of simulated gas flow at changed barometric pressures were placed in Appendix 1. These results indicate that differences in barometric pressure have an insignificant effect on pipe gas velocity or the general direction or pattern of dump gas flow.

3.3 *Transient Gas Flow Conditions*

In order to investigate transient conditions in the dump following changes in temperature and barometric pressure, simulation printouts were generated every 5 minutes for a total time of 1 hour after the start of simulation. Figures 9 and 10 respectively show the evolution of pipe gas velocity and total gas mass in the dump after the initial “perturbation” corresponding to the start of a simulation. These figures show that after 15-20 minutes near steady state conditions are reached corresponding to the imposed atmospheric conditions. In the case of pipe gas velocities, the initial magnitudes at the onset of a simulation are very large and there can be reversals in flow direction at the start of a simulation compared to the direction reached at steady state. In the case of the total gas mass, the relative magnitude of the change is quite small, partially explaining why the transient period does not last long, along with the fact that gas exchanges through the pipe can rapidly transfer the gas mass required to reach the new steady state. These results demonstrate that the system can rapidly reach steady state conditions, even after the major perturbations imposed in numerical simulations. In the actual system, atmospheric conditions are progressively changing, rather than being subject of sudden variations. The short time required to reach steady state in simulations indicate that the system can dynamically adapt to progressive changes in atmospheric conditions. It would thus be uncommon to observe reversals in pipe flow direction due to changes in barometric pressure in the actual system, and any such changes would be short-lived.

3.4 *Gas Flow without a Till Cover*

In order to further investigate the role of the till cover on dump gas flow, simulations were carried out without a cover at 5 and 36 °C atmospheric temperatures. These simulations are meant to serve as basis for comparison to the base case. The material for till cover elements was replaced by waste rock, but these simulations otherwise use the same conditions applied to the base case, including the same mean internal dump temperature. This also includes the presence of the high permeability toe drain, even though this drain was in fact filled following cover placement. These simulations are not necessarily representative of the conditions that would actually prevail without a cover, but rather aim at better understanding the role of the cover under the conditions prevailing in the No. 1 Shaft Dump. These simulation results, especially gas

velocities, should thus only be interpreted relative to those obtained for the base case. If these simulations were carried out to represent actual conditions without a cover, it would then be important to consider more representative thermal conditions. Without a cover, the dump could have much more heat production due to the increase in oxygen supply, which would probably lead to higher mean temperatures.

Figure 11 compares gas flow patterns obtained with and without a cover at 5 °C under steady state. The scale of gas velocity vectors was changed compared to previous similar figures to better show gas flow patterns. The same scale is also used in both figures to facilitate comparison. Through most of the dump, velocities are higher without a till cover than with a cover, especially in the lower internal part of the dump. Gas entry or exit preferentially occurs at the base of the large dump slope. Table 7 shows that without a cover, pipe gas velocity is significantly higher than with a cover, at both 5 and 36 °C. Even though there is higher flow through the pipe, there is relatively less flow entering or leaving the dump through the pipe than elsewhere across the dump surface. These results have the important implication that even without a till cover, a dump in otherwise similar conditions as the No. 1 Shaft Dump would still have gas flow through a pipe at the base of the dump and would still be a personnel security threat when gas flow is downward, i.e. out of the pipe. Without a till cover, gas exchanges between the dump and atmosphere are unhindered, so transient conditions only last about 20 seconds, based on simulation printouts obtained every 10 seconds. Without a till cover, dump gas flow thus equilibrates almost instantaneously with changes in atmospheric conditions. These results show that even though the till cover allows enough gas flow to make buoyancy-driven gas convection possible in the dump, the presence of the cover still hinders gas exchanges between the dump and atmosphere.

3.5 Gas Flow without a Pipe

Again for comparison purpose, in order to further assess the importance of the pipe on gas exchanges, other numerical simulations were carried out without linking the pipe to the atmosphere at 5 and 36 °C atmospheric temperatures, with a dry and wet till cover. As the previous simulations without a cover, these simulations are meant to serve as basis for comparison to the base case. Besides the absence of link between the pipe and atmosphere, these

simulations use the same conditions applied to the base case, including the same mean internal dump temperature. Contrary to previous simulations without a cover, these simulations without a pipe could actually be representative of conditions that could prevail without a pipe. The time required to reach the present-day mean internal dump temperatures observed in the No. 1 Shaft Dump could be shorter without a pipe due to the likely lower air and oxygen supply to the dump.

Figure 12 shows simulation results at 5 and 36 °C for a dry till cover (compare to base case shown on Figure 6). Without a pipe, gas flows through the dump surface, rather than the pipe, in the lower part of the dump. This leads to lower velocities in the dump, especially in its lower part as shown in Table 4c. Despite lower velocities, gas flow patterns are otherwise similar as the ones obtained for the base case. These results show that even without the pipe similar gas flow circulation would occur under the conditions prevailing in the No. 1 Shaft Dump. However, these results also show that the pipe offers a preferential path facilitating gas exchanges between the dump and atmosphere. Without this preferential path, gas exchanges between the dump and atmosphere would be reduced and there would be less gas flow through the dump.

4. Discussion on Processes Controlling Gas Flow

4.1 Pneumatic Potential Controlling Gas Flow

Monitoring data and numerical modeling of the No. 1 Shaft Waste Rock Dump show that gas flow in that dump is controlled by atmospheric temperature. The physical process depending on temperature that is at the origin of gas flow is thermal convection due to dump gas buoyancy. Dump gas buoyancy depends on its density relative to atmospheric air. Gas (or air) density ρ_a (kg/m³) is obtained from the following relations derived from the gas law (Lefebvre, 2006):

$$\rho_a = \frac{M}{V} = \frac{nm}{V} = \frac{pm}{RT'} = \frac{p \sum (x_i m_i)}{RT'} \quad 1$$

Where M (kg) and V (m³) are respectively the mass and volume of gas. The mass of gas depends on its number of moles n (mol) and its molar mass m (kg/mol). The molar mass of a gas such as atmospheric air, which is a mixture of components i , is the sum of the products of molar fractions x_i and molar masses m_i of these components. The volume of gas is obtained from its pressure p (Pa) and absolute temperature T' (K) and the gas constant R (8.31 Pa·m³/mol·K).

In the case of the No. 1 Shaft Dump, it was already mentioned that the molar mass of dump gas is similar to the one of atmospheric air. Also, under steady state equilibrium, the mean gas pressure is fixed at a similar value by the prevalent barometric pressure both in the atmosphere and within the dump. The difference between dump gas and atmospheric air densities thus only depend on their respective temperature, gas density being inversely proportional to temperature.

The dump maintains a relatively steady mean internal temperature of about 10-12 °C that it imparts to the gas phase present within the dump (Section 2.1, Figure 3). However, atmospheric temperature is quite variable, so that the density of the atmospheric air in contact with the dump will vary. Based on these principles and as shown by simulation results, in the case where atmospheric temperature is similar to the mean dump temperature, the density of atmospheric air will be the same as the one of dump gas and there will be no tendency for dump gas to flow. This is referred in this report as the “equilibrium temperature”. However, when atmospheric

temperature is lower than dump temperature, its density is higher than dump gas, which will tend to rise up through the atmosphere (positive buoyancy). On the contrary, when atmospheric temperature is higher than dump temperature, its density is lower than dump gas, which will tend to sink down through the atmosphere (negative buoyancy).

This process of buoyancy-driven gas flow controlled by atmospheric temperature departures from the dump “equilibrium temperature” is in qualitative agreement with the measured directions and magnitudes of pipe gas velocity versus atmospheric temperature. For this gas circulation process to occur, there has to be flow through the till cover and waste rock in the dump. The pipe directly connects the dump to the atmosphere, but flow also has to go through the dump top surface or through defects in the till cover. If the till cover were “perfectly” impermeable, the gas flow behavior would be quite different. Pressure equilibration between dump gas and the atmosphere would only occur by gas circulation through the pipe. However, there would be zero gas flow under steady state after pressure equilibration. Furthermore, flow through the pipe would be linked to barometric pressure changes, rather than atmospheric temperature variations. Thus, the strong relation of pipe gas velocity with atmospheric temperature and the insignificant effect of barometric pressure provide strong indirect indications that significant gas flow can occur through the dump surface.

The magnitude of dump gas flow through the dump is driven by the difference in pneumatic potential between the top and base of the dump that is caused by the buoyancy of dump gas relative to atmospheric air. The numerical simulator rigorously takes into account all processes contributing to gas flow as well as the compressibility of the gas phase. However, the simulator does not provide as an output the values of the pneumatic potential. These potentials much better show the processes controlling dump gas flow and gas exchanges between the dump and atmosphere than gas pressure. Thus, for the purpose of generating graphs, the following simplified form of the pneumatic potential Ψ (Pa) was calculated using numerical modeling results (Lefebvre, 2006):

$$\Psi = \rho \cdot g \cdot (z - z_0) + p \quad 2$$

Equation 2 is analog to the definition of hydraulic head, with a component of gas pressure p (Pa) and a component of elevation, which is the product of gas density ρ (kg/m^3), gravitational acceleration g (9.81 m/s^2) and elevation difference between the pressure measure point z (m) and an arbitrary reference elevation z_o (m) (elevation is positive upward). This relationship is neglecting gas compressibility, i.e. that density varies with pressure as shown by equation 1. However, over the short vertical interval of the No. 1 Shaft Dump, there is a very small change in density related to elevation and pressure. Pneumatic potentials were thus calculated “inside” the dump using the mean dump gas density corresponding to the mean internal dump temperature and pressure. The same relationship was also used for the surface boundary elements corresponding to atmospheric conditions. Pneumatic potentials for boundary atmospheric conditions indicate if atmospheric pneumatic potentials are in equilibrium with dump gas or would rather induce upward or downward dump gas flow.

Table 1 shows the pneumatic potential values calculated at the dump top surface and the pipe for the minimum, mean (equilibrium) and maximum atmospheric temperatures encountered at the site. The table also lists the mean dump gas and atmospheric air densities at these temperatures. The differences in density between dump gas and atmospheric air indicates that dump gas flow should generally be upward and downward, at respectively low and high atmospheric temperatures. The magnitude of that flow will depend on the pneumatic potential differences between the top of the dump and the pipe. The direction of dump gas flow is also shown by the fact that pneumatic potential is lower than at the pipe under low atmospheric temperature and higher at high temperature.

Respectively for simulations at atmospheric temperatures of $5 \text{ }^\circ\text{C}$ and $36 \text{ }^\circ\text{C}$, Figures 13 and 14 show calculated pneumatic potentials corresponding to simulated conditions. Each figure shows conditions for three simulated cases: the base case with dry till cover and pipe, the case with dry till cover and no pipe, and the case without till cover but with pipe. The simulated high and low barometric pressure cases are not illustrated as these results are very similar to the base case, but with shifted absolute values of pneumatic potential. Figures 13 and 14 also show streamlines indicating gas flow paths within the dump. Arrows along these streamlines indicate the flow direction, whereas black squares are time markers whose spacing indicates 5 day flow duration.

White squares on the graphs indicate the four representative locations within the dump for which gas velocities are reported in Table 4.

The top graphs of Figures 13 and 14 represent simulated conditions for the base case, respectively at 5 and 36 °C. Although dump gas flows in opposite directions at these different atmospheric temperatures, gas flow patterns have common features. First, most of the gas exchanges between the dump and atmosphere occur through the pipe (and toe drain) and the top surface of the dump. This is indicated by the fact that a vast majority of streamlines extends from the pipe to the top surface of dump. The area of the pipe and toe drain within the dump has a potential similar to the one of the dump surface boundary at atmospheric conditions. However, there is a large potential difference between the uppermost part of the dump and the boundary at the top dump surface (shown by the contrast in color representing potential magnitude). This indicates that a significant loss in potential occurs as gas flows across the till cover at the dump top surface. This feature is also apparent on the graphs of pneumatic potential versus elevation shown on Figure 15 that will be discussed later. There is limited exchanges through the till cover along dump slope as indicated a few streamlines originating from the slope. On that slope, gas is exchanged in different directions through the till in the upper and lower parts of the dump slope.

Table 4a shows that gas velocities are low in the interior and top portion of the dump, become higher in the center of the slope and are the fastest in the lower thin portion of the dump. This is also qualitatively indicated by the spacing of streamline time markers on Figures 13 and 14: farther apart markers indicate faster gas flow. Since little flow occurs through the till cover, there is about the same total gas flow rate from the top dump surface to the pipe located at the base of the dump. Gas velocity is thus related to the available gas flow cross section through the dump, which is much larger in the thick upper part of the dump than in the lower thin portion near the base of the dump. Gas velocities are higher for the case at low atmospheric temperature (5 °C) than at high temperature (36 °C) (Table 4a). This is due to the higher difference in pneumatic potential between the dump top surface and the pipe at 5 °C compared to 36 °C (Table 2). These differences in gas velocity between these two cases influence the total gas transit time through the dump. The transit time actually depends of the position within the dump. For the case at 5 °C, if atmospheric temperature remained constant, it would take more than a month for gas to transit

through the lower part of the dump, whereas the transit time would be less than 20 days through the upper portion of the dump closer to the slope. In the case of the gas transiting across the dump slope, its transit time would be less than 10 to 15 days. Since gas flow is slower for the 36 °C case, the total transit time would take more than 2 months in the lower part of the dump and in the order of 40 days in the upper portion of the dump close to the slope.

The middle graphs of Figures 13 and 14 show potentials and streamlines for the simulation case without a pipe, respectively at 5 and 36 °C atmospheric temperatures. Compared to the base case, the absence of a pipe results in the same general flow direction and quite similar gas flow patterns through the dump. Without a pipe, the main difference compared to the base case is that gas has to flow through the till cover in the lower part of dump. There is an important potential loss as gas flows through the till (shown by the contrast in color related to potential magnitude). This is also apparent in Figure 13 that will be discussed later. Table 3c also indicates that gas velocity is decreased compared to the base case in lower part of dump. This is caused by more restricted gas exchanges between the dump and atmosphere in the absence of the pipe. As mentioned before, results for simulations without a pipe should only be compared to the base case as they are not meant to represent what would actually occur without a pipe, but rather what is the role of the pipe under the conditions presently prevailing in the dump.

The lower graphs of Figures 13 and 14 show potentials and streamlines for the simulation case without a till cover, respectively at atmospheric temperatures of 5 and 36 °C. Compared to the base case, the absence of till cover leads to much faster gas flow in the dump. Since there is no till cover, in this case there is no potential loss across the dump surface. This leads to increased gas entry in the dump through the slope as well as the pipe. However, gas entry through the pipe is relatively less important, compared to gas entry through the slope. This is indicated by the fact that less streamlines are transiting through the pipe than what occurred for the base case. Table 3d shows that gas velocities are all higher through the dump than in the base case, except through the lower part of the dump. Again, results for simulations without a cover should only be compared to the base case as they are not meant to represent what would actually occur without a cover, but rather what is the role of the cover under the present conditions of the dump.

Figure 15 presents graphs of pneumatic potential versus elevation in the dump for simulated conditions prevailing after 12 hours, i.e. near steady state. Under these conditions there is equilibrium between imposed atmospheric temperature and pressure on the dump and gas flow within the dump. The three main simulation cases are presented: base case, no pipe, no cover. The high and low barometric pressure cases are not illustrated as they are very similar to the base case, but with shifted absolute values of potential. Table 2 showed that imposed atmospheric conditions lead to pneumatic potential gradients between the top surface of the dump and the pipe. On Figure 15, the potentials related to boundary atmospheric conditions appear as linear trends spanning the entire dump elevation range. For a given atmospheric temperature, these trends are the same for all three simulation cases since boundary conditions are identical for these cases. These linear vertical pneumatic potential gradients at the dump surface control the direction of dump gas flow. For low atmospheric temperature (5 °C), the imposed boundary pneumatic potentials decrease with elevation, which leads to upward gas flow, whereas at high atmospheric temperature (36 °C), the imposed potentials increase with elevation, which imposes downward gas flow.

The top graphs of Figure 15 correspond to the base case. Since there is a direct link between the dump and the atmosphere provided by the pipe and toe drain, the lower part of dump gas has the same pneumatic potential as the atmosphere. As gas flows through the dump, there is a pneumatic potential loss in the flow direction, upward for the 5 °C case and downward for the 36 °C case. This loss is more important (higher gradient) in the lower part of dump where the flow cross section is restricted, whereas very little potential loss occurs in the upper thick part of dump. The dump gas pneumatic potentials cross the atmospheric values at an elevation of about 1320 m. Above and below that elevation, the difference in potential between the atmosphere and dump gas leads to limited gas exchanges across the till cover due to its low effective air permeability. There is a large difference in potential between the atmosphere and dump gas at the top of the dump that corresponds to the potential loss occurring while gas flows through the till cover at the top surface of the dump.

The central graphs of Figure 15 show the trends in pneumatic potential with elevation for the cases without a pipe. The main difference relative to the base case is that the upper and lower

ends of the dump are at different pneumatic potentials than the atmosphere. Under these conditions, there are thus large potential losses as gas flows through the till cover at the base and upper portion of the dump slope, to either enter or exit the dump. The lower graphs of Figure 15 show conditions for the cases without a till cover. This time the main difference compared to the base case is that dump gas potentials are the same as atmospheric potentials along the entire slope of the dump. In the absence of cover, there is no potential loss as gas flows through the dump surface, which leads to overall larger dump gas potential gradient from the base to the top of the dump. This induces larger overall gas flows through the dump and more important gas exchanges between the dump and atmosphere without a till cover.

4.2 Gas Flow Conceptual Model

Table 8 summarizes the monitored conditions in observation boreholes, whose locations are shown on Figure 1 and projected positions on the numerical grid are indicated on Figure 4. The conditions compiled on Table 8 correspond to observations until the time the monitoring data were reviewed in December 2007. These conditions provide indications of gas flow conditions prevailing in the No. 1 Shaft Dump. On that basis, a gas flow conceptual model was developed, which guided the development of the numerical model used to simulate dump gas flow. That conceptual model is presented here so that the observations that formed the basis for its development can be compared to numerical simulation results. Such a comparison further validates the numerical model and ties together numerous observations made on conditions prevailing in the No. 1 Shaft Dump. Besides the conditions presented in Table 1, thermal conditions prevailing in the dump and gas densities estimated from boreholes gas compositions were also considered in the development of the conceptual model (Section 2.1).

Observed thermal conditions are the first data compiled in Table 8. Atmospheric temperature is presented as a reference and the values quoted for “Low”, “Mean” and “High” temperature are those obtained from a sinusoidal fit to the meteorological temperature data (Section 2.1). Values of borehole monitored parameters are representative of these different atmospheric temperature ranges. Temperature in boreholes listed in Table 8 is derived from measured monthly profiles that are affected by cyclic yearly air temperature variations as discussed in Section 2.1 (Figure 2). Boreholes BH-1A and BH-1B are the only ones deeper than the range affected by cyclic

yearly air temperature variations (about 10 m). Below 5 m depth, temperatures range from about 8 to 16 °C, with average values between about 10 to 14 °C (Figure 3).

Table 8 also compiles gas compositions observed in boreholes, which were found to be quite variable seasonally. Boreholes BH-1A and BH-1B have more stable gas compositions with low oxygen (1-5 %) and high CO₂ (4-6%). At low temperatures, oxygen concentrations are slightly higher, whereas CO₂ concentrations are lower. BH-2A has very low oxygen (1%) and very high CO₂ (10%) concentrations. This borehole may be isolated from the main gas flow system. BH-2B, BH-3A and BH-3B have widely varying seasonal gas concentrations, with high oxygen (can even be atmospheric) and low CO₂ under low air temperatures and almost no oxygen and high CO₂ (can exceed 12%) under high air temperatures. Representative values of gas densities calculated for the temperatures and gas composition found in boreholes are compared to atmospheric air densities (Section 2.1).

Finally, Table 8 compiles the differential gas pressures (dP) measured in boreholes, which provide indications of vertical gas flow tendencies. The measurements made when borehole gas was sampled are the ones shown in the table. The convention used for dP measurements is atmospheric pressure minus borehole pressure. Positive values of dP thus indicate downward flow tendencies, whereas negative values show upward flow tendencies. The data compiled indicate that both the sign and magnitude of dP vary seasonally. In boreholes at the top of the dump, BH-1A and BH-1B, dP indicates mostly upward gas flow, except when air temperature is high (above about 20 °C). The magnitude of dP is relatively low for these boreholes. The reverse behavior in dP is seen in other boreholes lower down the dump: dP indicates downward flow under cold conditions and upward flow under warm conditions, with relatively clear changes in direction with seasons at threshold values in the range of 12-13 °C. Monitored differential pressures are not coherent with measurements made when borehole gas was sampled.

Figure 16 compares numerical simulations for the low and high temperature base cases with the conceptual model of gas flow in the No. 1 Shaft Dump based on monitoring data. The conceptual model is based on observed differential pressures and gas compositions in observation wells and

from pipe velocities (Table 8). Both at low and high atmospheric temperature, the assumptions of the conceptual model are supported by numerical results.

At low atmospheric temperature, air enters the pipe, then gas flows laterally at fast velocity in the lower part of the dump, then slowly upward in the upper part of the dump. This generally upward flow tendency was assumed in the conceptual model on the basis of air entry in the pipe and differential pressures measured at the top of the dump indicating upward flow (Table 8). Lateral gas flow in the lower and central part of the dump was supported by the temperature profiles measured in observation wells that indicated heat production, thus oxygen supply and gas flow, over the entire thickness of the dump (Section 2.1). The large air inflow in the lower part of the dump was also supported by high oxygen concentrations observed in that part of the dump (Table 8). Lower gas velocities in the upper part of the dump were assumed on the basis of the dump geometry and the low oxygen concentrations observed in the upper part of the dump. The model also supports the tendency for gas to flow downward through the till cover in the lower part of the dump and upward flow in the upper part of the dump (Table 8). These flow tendencies were deduced from pressure gradients observed in boreholes located in the upper and lower portions of the dump slope (Table 8). The numerical model only contradicts the conceptual model about the assumed gas entry through the till cover in the upper part of the slope that was assumed on the basis of gas composition, i.e. the presence of oxygen.

At high temperature, dump gas exits through the pipe, there is rapid lateral gas flow in the lower part of the dump, and slow gas flow in the upper part of the dump. This pattern was again inferred from pipe gas flow and pressure gradients observed on the top of the dump (Table 8). The strong lateral gas flow in the lower part of the dump was also indicated by oxygen-depleted and CO₂-rich composition of dump gas flowing through the pipe. Such a composition shows that air has not significantly entered the dump along the gas flow path and that gas comes from within the dumps where oxygen is consumed and CO₂ produced. The tendency for gas entry and exit through the till cover, respectively in the lower and upper part of the dump slope, were again based on differential pressures measured in boreholes (Table 8). Numerical modeling results also support the assumption made that gas flux would be lower at the higher atmospheric temperatures relative to the lower ones.

These agreements between various monitoring observations with model predictions further validate the numerical model, which was shown to be calibrated on the basis of its predictions of pipe gas velocities as a function of temperature (Figure 7). However, the model does not represent the potential effects of heterogeneities in the waste rock and till cover. Such heterogeneities could lead to preferential gas flow paths and gas stagnation zones in the dump.

5. Conclusions

The numerical model developed to represent gas flow in the Sullivan Mine No. 1 Shaft Waste Rock Dump reproduces pipe gas velocities as a function of temperature and is in general agreement with monitoring observations. In order to calibrate the model, the effective air permeability of the till cover and waste rock had to be significantly increased from the initial estimates based on available data. It is presumed that the increased permeabilities required by the model reflect the combined effects of coarse preferential flow paths in waste rock and localized variability in the cover. There are probably other combinations of permeabilities for the till cover, waste rock and toe drain fill material that would have allowed model calibration. Representative results obtained from simulations support the simplifying assumptions made to develop the model, mainly that 1) the presence of CO₂ in the dump gas could make its molar mass equivalent to atmospheric air, 2) the mean dump temperature remains relatively constant, and 3) water flow in the dump does not significantly alter gas flow.

The physical process at the origin of gas flow in the dump is thermal convection due to dump gas buoyancy. The dump gas buoyancy depends on its density difference relative to atmospheric air. The difference between dump gas and atmospheric air densities only depend on their respective temperatures: the dump gas temperature remains quite constant whereas the atmospheric temperature is variable and thus controls gas flow direction and magnitude. The dump is supposed to maintain a relatively steady temperature of about 10-12 °C. When atmospheric temperature is similar to the mean dump temperature, there will be no tendency for dump gas to flow. However, when atmospheric temperature is lower than 10-12 °C, its density is higher than dump gas, which will tend to rise up through the atmosphere (positive buoyancy) and air will enter the pipe. On the contrary, when atmospheric temperature is higher than 10-12 °C, its density is lower than dump gas, which will tend to sink down through the atmosphere (negative buoyancy) and dump gas will exit the pipe. Under these conditions, the dump gas will tend to be less dense than the surrounding atmosphere in winter and denser during summer. Such a mechanism implies that gas flow is controlled by external forces, namely atmospheric temperature, rather than by the properties of its cover or waste rock, as long as these materials are permeable enough to allow buoyancy-driven gas flow to occur.

Gas flow in the dump is not significantly affected by barometric pressure changes as it does not significantly affect the relative density of dump gas and atmospheric air. The pipe and high permeability toe drain fill material facilitate gas flow and exchanges with the atmosphere. The system was found to rapidly reach steady state gas flow conditions, in about 15 minutes, even following major perturbations in atmospheric temperature and pressure. Gas flow through the pipe and till cover can rapidly provide the relatively small gas volume required to compensate the effects of simulated atmospheric temperature and pressure changes. The natural system does not undergo such drastic changes and the system is dynamically reaching a new equilibrium related to variations in atmospheric conditions.

Most of the gas flowing through the dump enters or exits through the pipe. However, there would still be similar gas flow patterns without the presence of the pipe. Similarly, although the till cover restricts gas exchanges between the dump and the atmosphere, a low permeability cover is not required to obtain the observed gas flow behavior. Actually, there would even be more gas flow without a cover and gas would similarly flow through the pipe. A perfectly sealing dump cover would not lead to the observed gas flow behavior.

General conditions that could lead to a gas flow behavior similar to the one observed at the No. 1 Shaft Dump can be inferred from the characteristics of that dump and the processes that were shown to be controlling gas flow:

- Low mean internal dump temperature, within the range of yearly atmospheric temperature variations, so that dump gas and atmospheric air densities have the possibility to be similar. For example, such low dump temperatures could occur in low reactivity dumps, moderate permeability dumps or covered dumps;
- The waste rock dump has to be permeable “enough” (waste rock and cover combined) to allow buoyancy-driven gas convection to dominate exchanges in gas flow between the dump and atmosphere;
- A relatively large dump thickness would be favorable, as it would help maintain a steady internal dump temperature by avoiding too much influence from yearly atmospheric temperature variations;

- Geometry of the dump may play a role, as an important vertical component and sloping base may favor vertical gas flow related to buoyancy-induced convection (as shown for a Questa Mine waste rock dump by Lefebvre et al., 2002);
- The presence of CO₂ in the dump gas may not be necessary, but it facilitates the equilibrium between dump gas and atmospheric air densities by allowing dump gas molar mass to remain close to the one of atmospheric air;
- A filled toe drain and pipe are not necessary but their presence enhances gas flow, and the pipe poses the main security threat as it is focusing dump gas exit;
- Enclosures and topographic depressions bordering the base of a dump, where dense oxygen-deprived dump gas could accumulate, would represent hazard locations;
- The presence of a cover may not be necessary and it could even preclude the type of gas flow observed at the No. 1 Shaft Dump. However, covered dumps have limited oxygen supply and may tend to steadily reduce their internal temperatures, which would lead to conditions favorable to the onset of gas flow conditions as observed at the No. 1 Shaft Dump.

The conditions listed are not meant to be all inclusive. Further work would be required to assess the full range of conditions that could lead to a gas flow behavior similar to the one observed at the No. 1 Shaft Dump, or to other gas flow behaviors that would also represent a security threat. This issue is complex as there is a wide range in dump gas composition, waste rock air permeabilities, dump geometries, and atmospheric conditions, which could influence gas flow and thus need to be considered.

6. References

Kimberley Incident Technical Panel, 2007. Update on technical findings. June 2007, 15 p.

Lahmira, B., Lefebvre, R., Aubertin, M., Bussière, B., 2007. Modeling the influence of heterogeneity and anisotropy on physical processes in AMD-producing waste rock piles. Proceedings, *OttawaGeo 2007, 60th Canadian Geotechnical Conference and 8th Joint CGS/IAH-CNC Groundwater Conference*, Ottawa, Canada, October 21-24, 8 p.

Lefebvre, R., 2006. Écoulement multiphase en milieux poreux. Graduate course notes, 6^e éd., GEO-9602/GLG-65146, Joint Graduate program, Laval University / INRS-ETE, INRS-Eau, Terre et Environnement, 371 p. et annexes.

http://www.ete.inrs.ca/professeur.php?page=ReneLefebvre_Enseignement

Lefebvre, R., Lamontagne, A., Wels, C., Robertson, A. MacG., 2002. ARD Production and Water Vapor Transport at Questa Mine. *Tailings and Mine Waste '02*, Proceedings of the Ninth International Conference on Tailings and Mine Waste, Fort Collins, Colorado, 27-30 January 2002, A.A. Balkema Publishers, 479-488.

Lefebvre, R., Lamontagne, A., Wels, C., 2001c. Numerical simulations of acid rock drainage in the Sugar Shack South rock pile, Questa Mine, New Mexico, U.S.A. Proceedings, *2nd Joint IAH-CNC and CGS Groundwater Specialty Conference, 54th Canadian Geotechnical Conference*, Sept. 16-19, 2001, Calgary, Canada, 1568-1575.

Lefebvre, R., Hockley, D., Smolensky, J., Lamontagne, A., 2001b. Multiphase transfer processes in waste rock piles producing acid mine drainage, 2: Applications of numerical simulations. *J. of Contaminant Hydrology*, 52 (1-4), 165-186.

Lefebvre, R., Hockley, D., Smolensky, J., Gélinas, P., 2001a. Multiphase transfer processes in waste rock piles producing acid mine drainage, 1: Conceptual model and system characterization. *J. of Contaminant Hydrology*, 52 (1-4), 137-164.

Lefebvre, R., Smolensky, J., Hockley, D., 1998. Modeling of acid mine drainage physical processes in the Nordhalde of the Ronnenburg mining district, Germany. Proceedings, *TOUGH Workshop '98*, Lawrence Berkeley National Laboratory, Berkely, CA, May 4-6, 1998, 6 p.

Lefebvre, R., G elinas, P.J., 1995. Numerical modelling of AMD production in waste rock dumps. Proceedings, *Sudbury '95 - Mining and the Environment Conference*, May 29-June 1, 1995, Sudbury, Canada, Paper NT2, v. 3, 869-878.

Lefebvre, R., 1995. Modeling acid mine drainage in waste rock dumps. In K. Pruess, ed., Proceedings, *TOUGH Workshop '95*, Berkeley, CA, March 20-22, 1995, Lawrence Berkeley Lab., LBL-37200, 239-244.

Phillip, M., Hockley, D. 2007. Sullivan Fatalities Incident – Technical Investigations and Findings. *14th Annual BC MEND Workshop*, Vancouver, BC, November 28, 2007.

Pruess, K., Oldenburg, C., Moridis, G., 1999. TOUGH2 user's guide, Version 2.0. Lawrence Berkeley National Laboratory, Report LBNL-43134, November 1999, 198 p.

Smolensky, J., Hockley, D., Lefebvre, R., Paul, M., 1999. Oxygen transport processes in the Nordhalde of the Ronnenburg mining district, Germany. Proceedings, *Sudbury '99 - Mining and the Environment II*, Sudbury, Ontario, Sept. 13-15, 1999, Paper AD 29, vol. I, 271-280.

Sracek, O., Choquette, M., G elinas, P., Lefebvre, R., Nicholson, R.V., 2004. Geochemical characterization of acid mine drainage from a waste rock pile, Mine Doyon, Qu ebec, Canada. *J. of Contaminant Hydrology*, 69 (1-2), 45-71.

Wels, C., Lefebvre, R., Robertson, A.M., 2003. An overview of prediction and control of air flow in acid-generating waste rock dumps. Proceedings, *6th International Conference on Acid Rock Drainage (ICARD)*, 12-18 July 2003, Cairns, Australia, Published by The AusIMM, Carlton South, VIC, Australia, 639-650.

Tables

Table 1. Estimated gas densities in monitoring boreholes compared to atmospheric air densities

	Atmosphere			BH-1 A&B			BH-2B			BH-3B		
	Low T	Mean T	High T	Low T	Mean T	High T	Low T	Mean T	High T	Low T	Mean T	High T
Temperature (oC)	-8	7.5	23	13.7	13.7	13.7	10	10	10	13	13	13
Oxygen vol. %	21.0%	21.0%	21.0%	3.0%	3.0%	3.0%	10.20%	3.90%	0.20%	8.50%	5.30%	1.20%
CO2 vol. %	0.03%	0.03%	0.03%	5.0%	5.0%	5.0%	1.90%	4.50%	6.70%	2.70%	4.30%	6.25%
Relative humidity	70%	70%	70%	100%	100%	100%	100%	100%	100%	100%	100%	100%
Saturated vapor pressure (Pa)	355	1056	2805	1581	1581	1581	1245	1245	1245	1512	1512	1512
Water vapor fraction	0.0041	0.0122	0.0323	0.0182	0.0182	0.0182	0.0144	0.0144	0.0144	0.0174	0.0174	0.0174
Dry gas molar mass	0.0290	0.0290	0.0290	0.0289	0.0289	0.0289	0.0287	0.0289	0.0291	0.0288	0.0289	0.0291
Humid gas molar mass	0.0289	0.0288	0.0286	0.0287	0.0287	0.0287	0.0286	0.0287	0.0289	0.0286	0.0287	0.0289
Gas density	1.137	1.071	1.008	1.045	1.045	1.045	1.052	1.058	1.066	1.042	1.047	1.052
DOWN	Relative density @ high atm. Temperature:			1.037			1.058			1.044		
UP	Relative density @ mean atm. Temperature:			0.975			0.988			0.977		
UP	Relative density @ low atm. Temperature:			0.918			0.925			0.916		

Note: the vertical direction of the waste rock dump gas flow should be UP when the relative density is lower than 1

Table 2. Temperature and pressure conditions with corresponding pneumatic potential

Imposed Conditions	Minimum atmospheric temperature (°C)	“Mean” dump temperature (°C)	Maximum atmospheric temperature (°C)
Real value	-8	12	23
Model value	5	25	36
Pressure at dump top ^a (Pa)	85 862	86 821	87 300
Pressure at pipe ^b (Pa)	86 498	87 415	87 869
Mean dump gas density (kg/m ³)	0.991	1.002	1.008
Mean atmospheric air density (kg/m ³)	1.062	1.002	0.972
Pneumatic potential ^c at dump top (Pa)	85 862	86 821	87 300
Pneumatic potential at pipe (Pa)	85 905	86 821	87 266
Potential difference (Top – Pipe) (Pa)	-43	0	34
Dump gas general flow direction	Upward	No flow	Downward

a: the top of the dump is at an elevation of 1348 m.

b: the pipe at the bottom of the dump is at an elevation of about 1287 m.

c: pneumatic potentials are calculated within the dump for conditions corresponding to the dump gas mean density at the internal dump temperature (25 °C) and gas pressure (using equation 2). The following relationships apply for the three atmospheric temperatures shown on the table for which distinct barometric pressures lead to different mean dump gas densities:

Potential @ 5 °C (reference elevation at dump top, 1348 m): $\Psi = p + 9.7209 \cdot (z-1348)$

Potential @ 25 °C (reference elevation at dump top, 1348 m): $\Psi = p + 9.8296 \cdot (z-1348)$

Potential @ 36 °C (reference elevation at dump top, 1348 m): $\Psi = p + 9.8838 \cdot (z-1348)$

Table 3. Material properties

Property	Dry Till	Wet Till	Waste Rock	Drain & Pipe
Total porosity (dim.)	0.295	0.295	0.33	0.45
Residual water saturation (dim.)	0.80	0.950	0.35	0.45
Hydraulic conductivity (m/s)	5.00E-06	5.00E-06	1.00E-04	1.00E-03
Estimated effective air permeability (m ²)	1.46E-13	9.41E-15	9.34E-12	1.02E-10
Used effective air permeability (m²)	5.10E-12	5.10E-12	5.02E-09	5.02E-05
Van Genuchten α parameter (Pa ⁻¹)	0.000008	0.000008	0.00085	
Van Genuchten m parameter (dim.)	0.55	0.55	0.3	
Van Genuchten n parameter (dim.)	2.22	2.22	1.43	

Table 4. Simulated gas velocities (m/d) in the waste rock dump
(Positive gas velocities are upward and negative values indicate downward flow)

<i>a) Base case with pipe linked to atmosphere</i>				
Location in the dump¹	5 °C	5 °C	36 °C	36 °C
	Dry Till	Wet Till	Dry Till	Wet Till
Interior base	+1.4	+1.4	-0.9	-0.9
Upper surface	+3.0	+3.0	-1.8	-1.8
Center of slope	+9.9	+9.6	-5.7	-5.7
Lower part	+23.1	+23.3	-12.7	-12.7

1: Locations in the dump are shown from left to right on Figures 11 and 12.

<i>b) Barometric pressure effect</i>		
Location in the dump	36 °C	36 °C
	Dry Till -2 kPa	Dry Till + 2 kPa
Interior base	-0.9	-0.9
Upper surface	-1.8	-1.9
Center of slope	-5.6	-5.8
Lower part	-12.4	-12.8

<i>c) Without pipe</i>		
Location in the dump	5 °C	36 °C
	Dry Till	Dry Till
Interior base	+1.2	-0.8
Upper surface	+2.6	-1.6
Center of slope	+7.7	-4.5
Lower part	+10.2	-6.0

<i>d) Without till cover</i>		
Location in the dump	5 °C	36 °C
	Interior base	+3.1
Upper surface	+6.9	-3.6
Center of slope	+29.4	-16.8
Lower part	+15.8	-8.6

Table 5. Simulated gas densities and velocities through the pipe
(Positive pipe gas velocities are inward and negative values indicate outward flow)

Model Atmospheric Temperature (°C)	Actual Atmospheric Temperature (°C)	Pipe Gas Density (kg/m ³)	Dry Cover Gas Velocity (m/s)	Wet Cover Gas Velocity (m/s)
5	-8	1.090	1.016	1.019
10	-3	1.069	0.779	0.781
15	2	1.048	0.533	0.534
20	7	1.025	0.274	0.275
25	12	1.001	0.000	0.000
30	17	0.975	-0.273	-0.274
35	22	0.946	-0.573	-0.575
40	27	0.914	-0.908	-0.912
45	32	0.878	-1.292	-1.297

Note: pipe open area is 0.1257 m²

Table 6. Simulated pipe gas velocities related to changes in barometric pressure at 36 °C

Cases	Normal Pressure at 36 °C		Increased Barometric Pressure (+2 kPa)		Decreased Barometric Pressure (-2 kPa)	
	Wet Till	Dry Till	Wet Till	Dry Till	Wet Till	Dry Till
Gas Density (kg/m ³)	0.940	0.940	0.961	0.961	0.918	0.918
Gas Flux (kg/s)	-7.55E-02	-7.52E-02	-7.86E-02	-7.83E-02	-7.24E-02	-7.21E-02
Gas Velocity (m/s)	-6.39E-01	-6.36E-01	-6.50E-01	-6.48E-01	-6.27E-01	-6.25E-01
Change in Gas Density (kg/m ³)			0.022		-0.022	
Change in Gas Velocity (m/s)			-1.152E-02	-1.169E-02	1.15E-02	1.15E-02
Change in Gas Velocity (%)			2.292		-2.290	

Table 7. Steady state pipe gas flow velocities without a till cover

Gas Velocity (m/s)		
Atm Temp	5°C	36°C
Dry Till	1.016	-0.636
Wet Till	1.019	-0.639
Without Till	1.800	-0.976
Difference (m/s)		
No Till - Dry Till	0.784	-0.340
No Till - Wet Till	0.782	-0.337

Table 8. Summary of monitored conditions in boreholes
(Conditions observed as of December 2007, when the numerical model was developed)

Borehole	Temperature (°C)	Oxygen (%)	CO ₂ (%)	Differential P Flow direction	Gas density (kg/m ³)	Remarks	
Atmosphere	Low T: Mean T: High T:	-8 7.5 23			1.137 1.071 1.008		
BH-1A	Low T: Mean T: High T:	10 13.7 16	2.3 1.2 1.1	4.4 5.1 5.7	Up fast at low T Mostly UP! Down >> 20 oC	1.060 1.045 1.035	
BH-1B	Low T: Mean T: High T:	10 13.7 16	2.5 3.2 4.8	4.5 4.5 4.5	Up fast at low T Mostly UP! Down >> 20 oC	1.060 1.045 1.035	One exceptional event of down flow at moderately "high" T
BH-2A	Low T: Mean T: High T:	7 10 13	1.3	10			No clear indication of flow direction on differential pressure (Borehole outside main flow path ???)
BH-2B	Low T: Mean T: High T:	7 10 13	10.2 3.9 0.2	1.9 4.5 6.7	Down when cold Up when hot	1.057 1.05 1.045	Getting O ₂ from air entry closer to monitoring borehole Gas can be near atmospheric under cold conditions... Evacuating gas without oxygen and high CO ₂ from "far" upstream
BH-3A	Low T: Mean T: High T:	8 11 14	11.7 7.7 0.3	2.1 4.4 8.6	Down when cold Up when hot		Gas can be near atmospheric under cold conditions... Stagnant gas (no flow) when atm. T about 12-13 oC High differential pressures (especially for upward flow)
BH-3B	Low T: Mean T: High T:	11 13 16	8.5 5.3 1.2	2.7 4.3 6.25	Down when cold Up when hot	1.043 1.039 1.032	Lower upward flow in moderate temperatures above 12 oC High differential pressures (especially for upward flow)
PIPE	Low T: Mean T: High T:		1 to 2	6.5 to 7	Flow IN Flow OUT		Atmospheric gas composition For initial short outflows: O ₂ rapidly decreasing and CO ₂ increasing For long and steady outflow: CO ₂ nearly constant and O ₂ slowly increasing

Similar - coherent - indications of flow directions and gas compositions in push in boreholes...

Figures

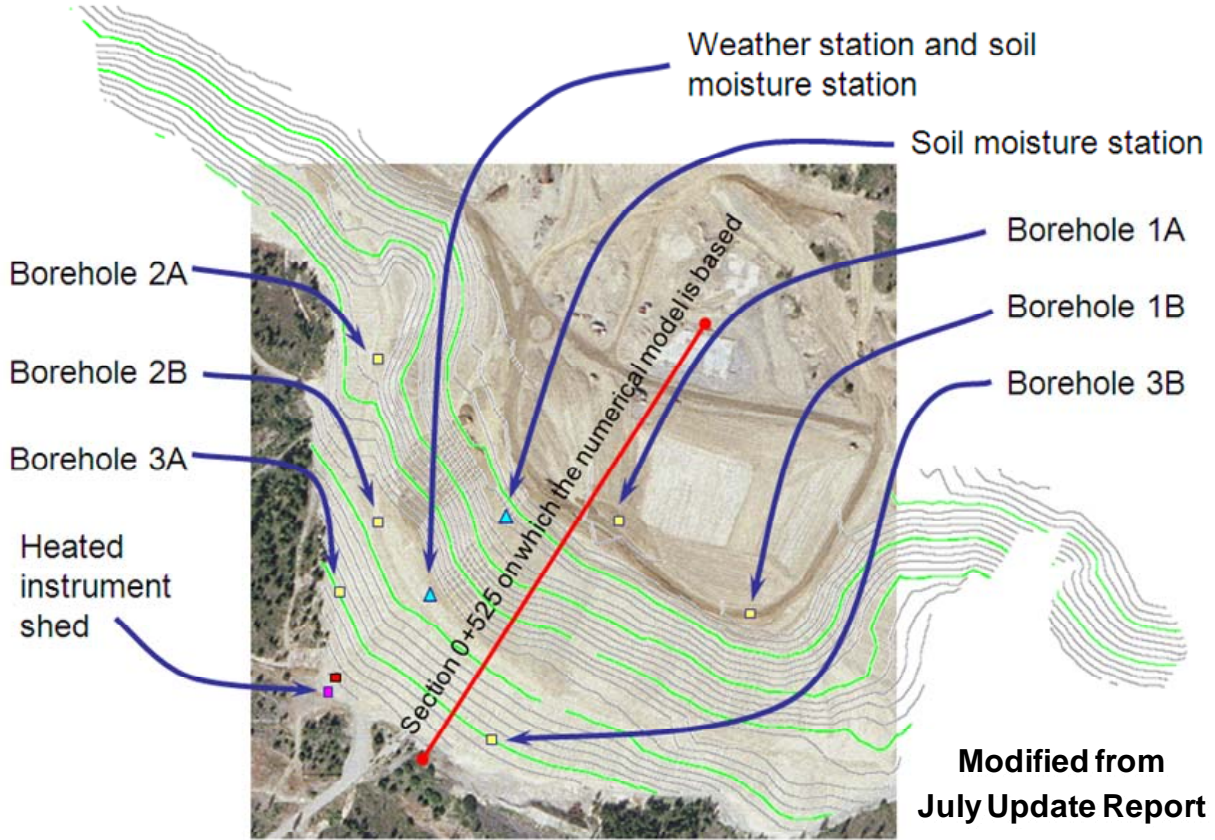


Figure 1. Location of Section 0+525 used to develop the numerical grid

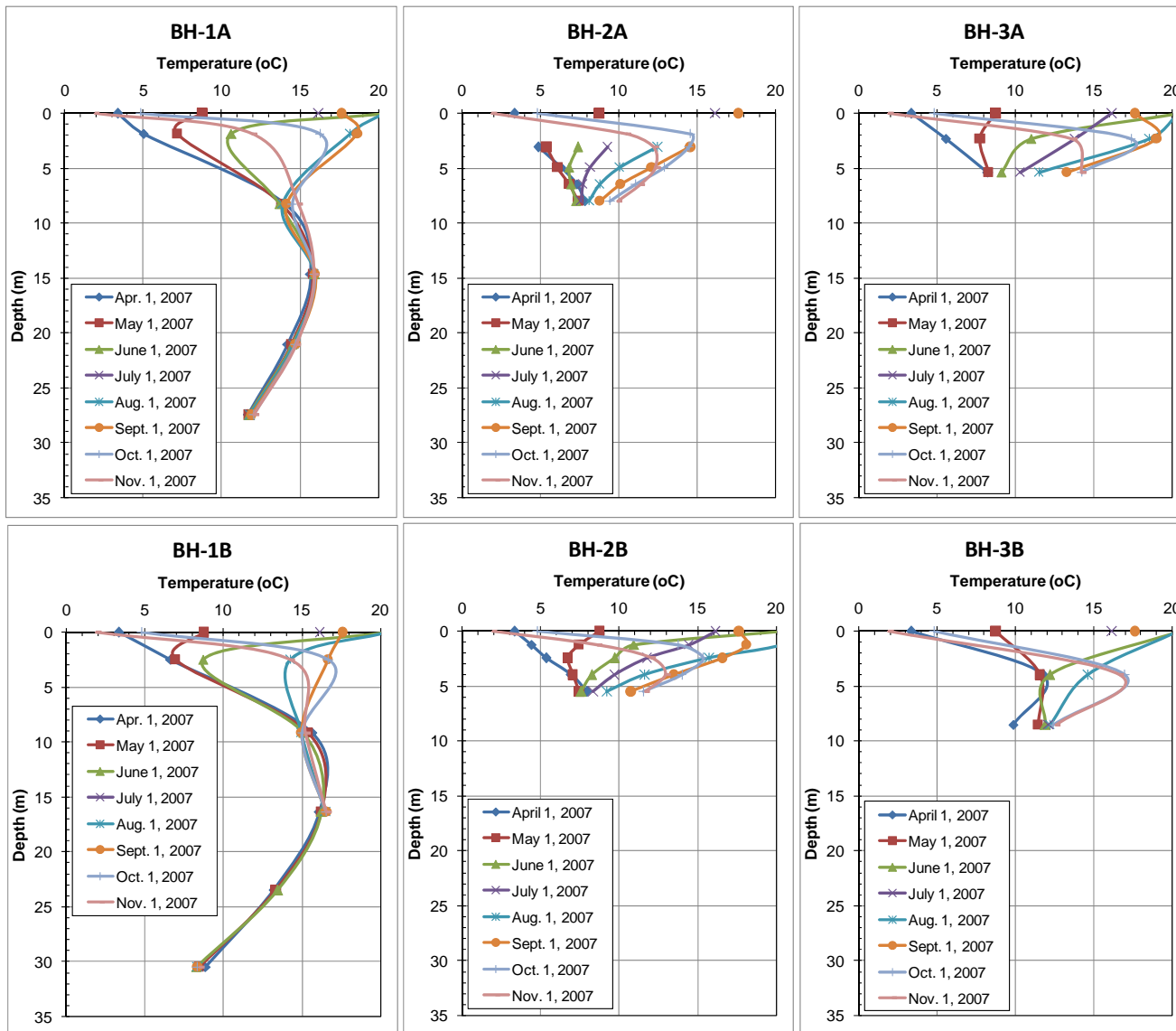


Figure 2. Selected monthly temperature profiles in boreholes

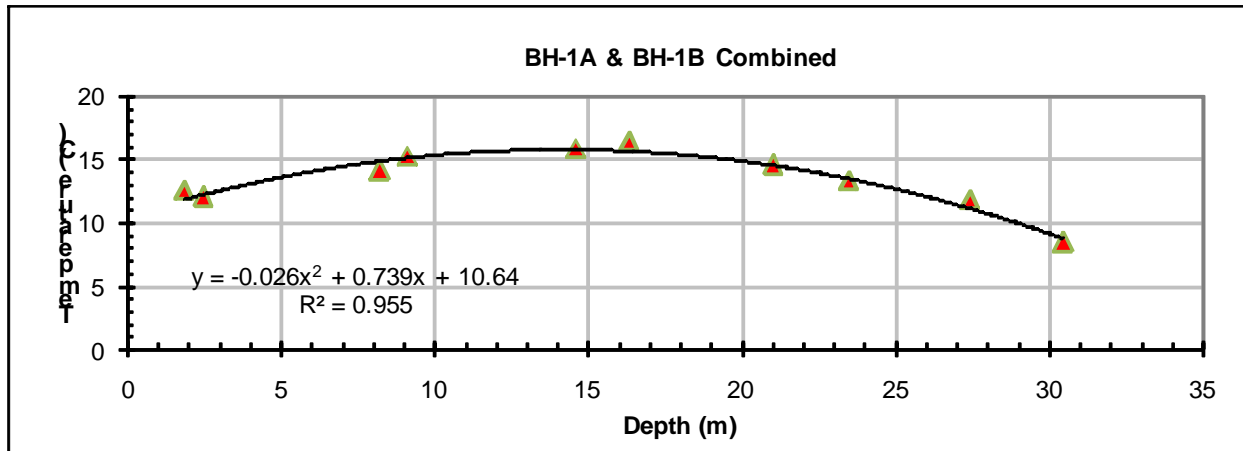


Figure 3. Second order polynomial fit to mean temperatures in boreholes BH-1A and BH-1B

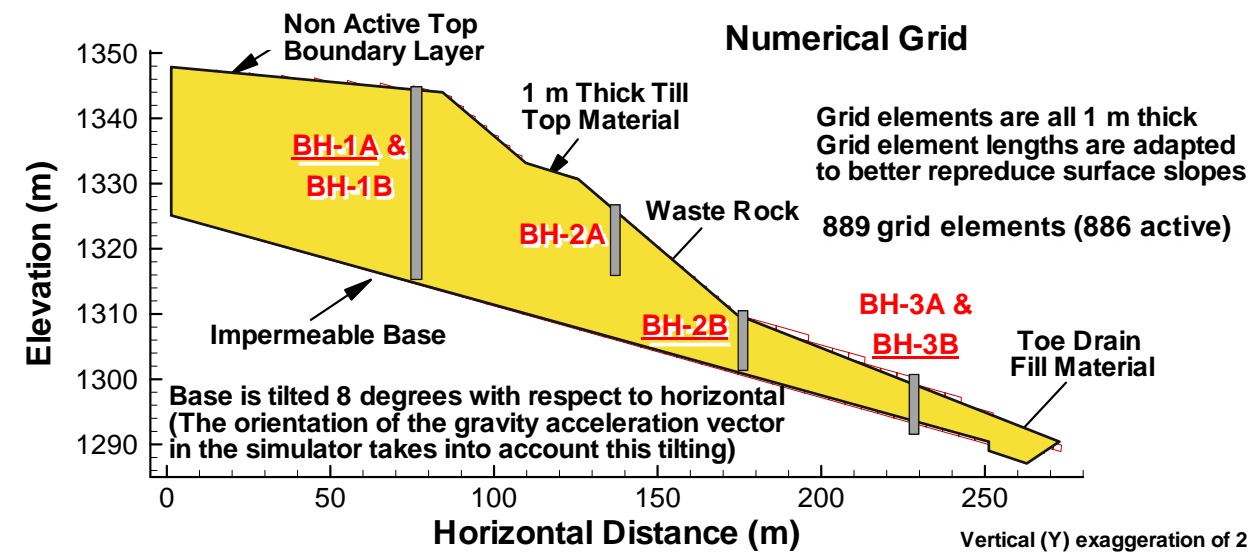


Figure 4. Projection of boreholes on the numerical grid section

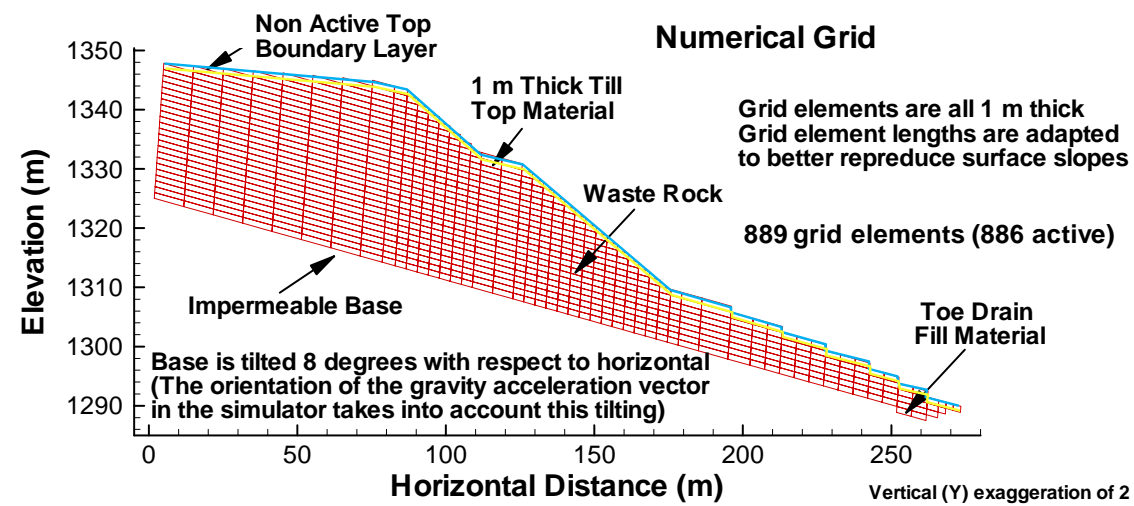


Figure 5. Boundary conditions and materials distribution in the numerical grid

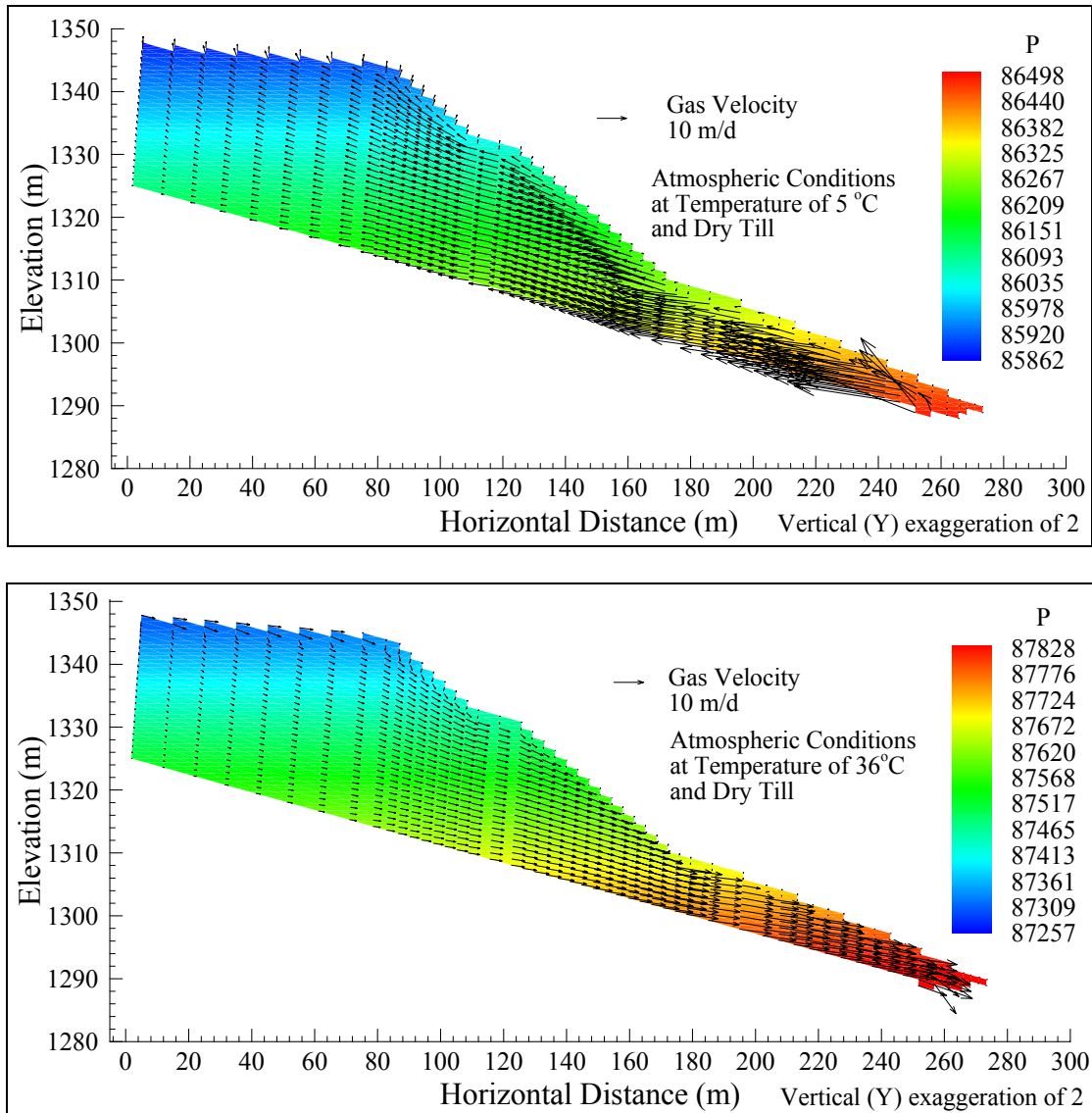


Figure 6. Simulated conditions for low (top) and high (bottom) atmospheric temperature. Simulations were made with the properties of the dry till cover. Arrows have lengths proportional gas velocity (m/d). The color scale represents gas pressure (Pa).

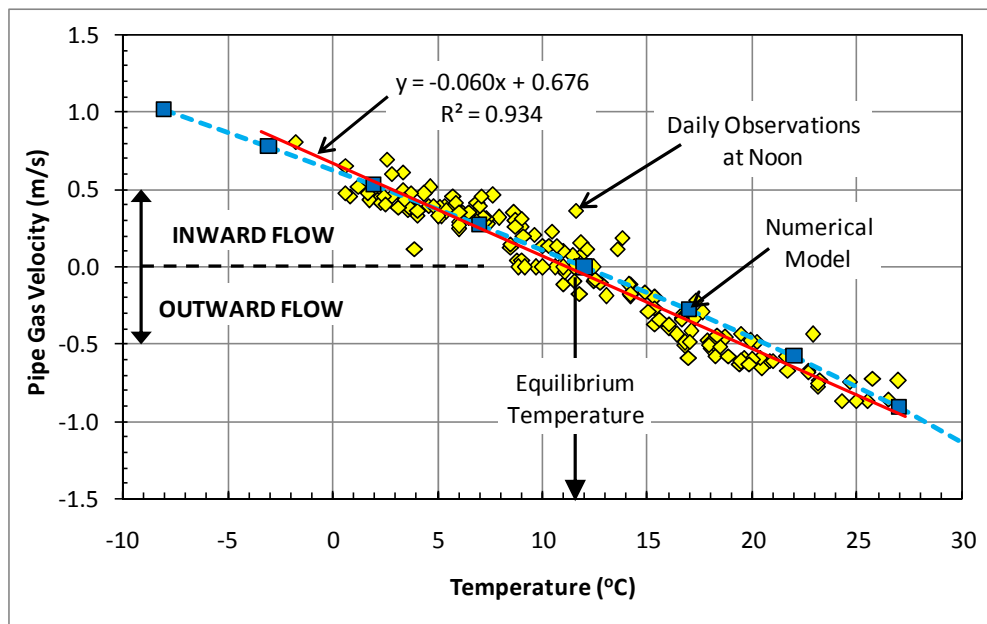


Figure 7. Comparison of simulated and measured gas velocities in the pipe. Positive pipe gas velocities correspond to gas flow in the pipe, whereas negative values represent gas flow out of the pipe. Simulations were carried out for a dry till cover at 5 °C interval above and below the equilibrium temperature. Simulation results (blue squares) are shown at temperatures of the actual system corresponding to simulation temperatures (Table 1). Observations shown (yellow lozenges) are selected daily values measured at Noon. The red line is the linear regression of observations. The dashed blue line linearly links simulation results

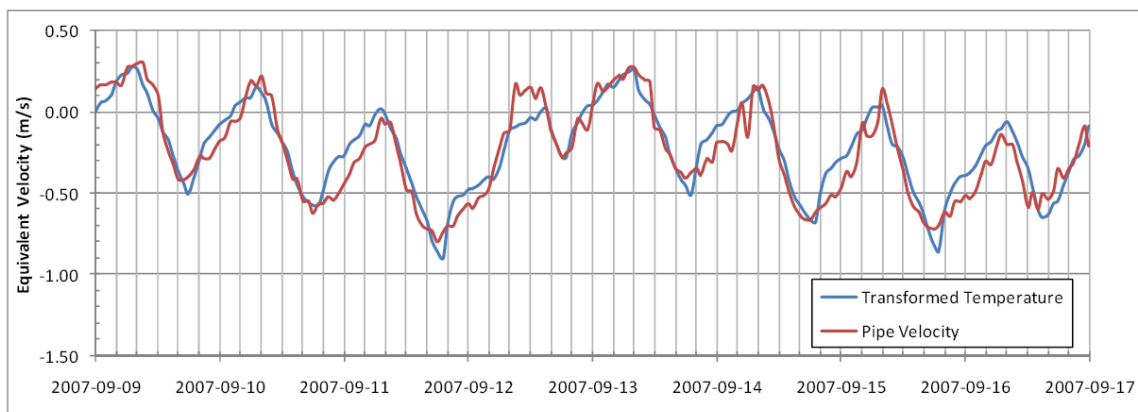


Figure 8. Correlation between normalized temperatures and pipe gas velocities. Normalized temperatures were calculated with the regression equation between temperature and pipe gas velocity shown on Figure 5

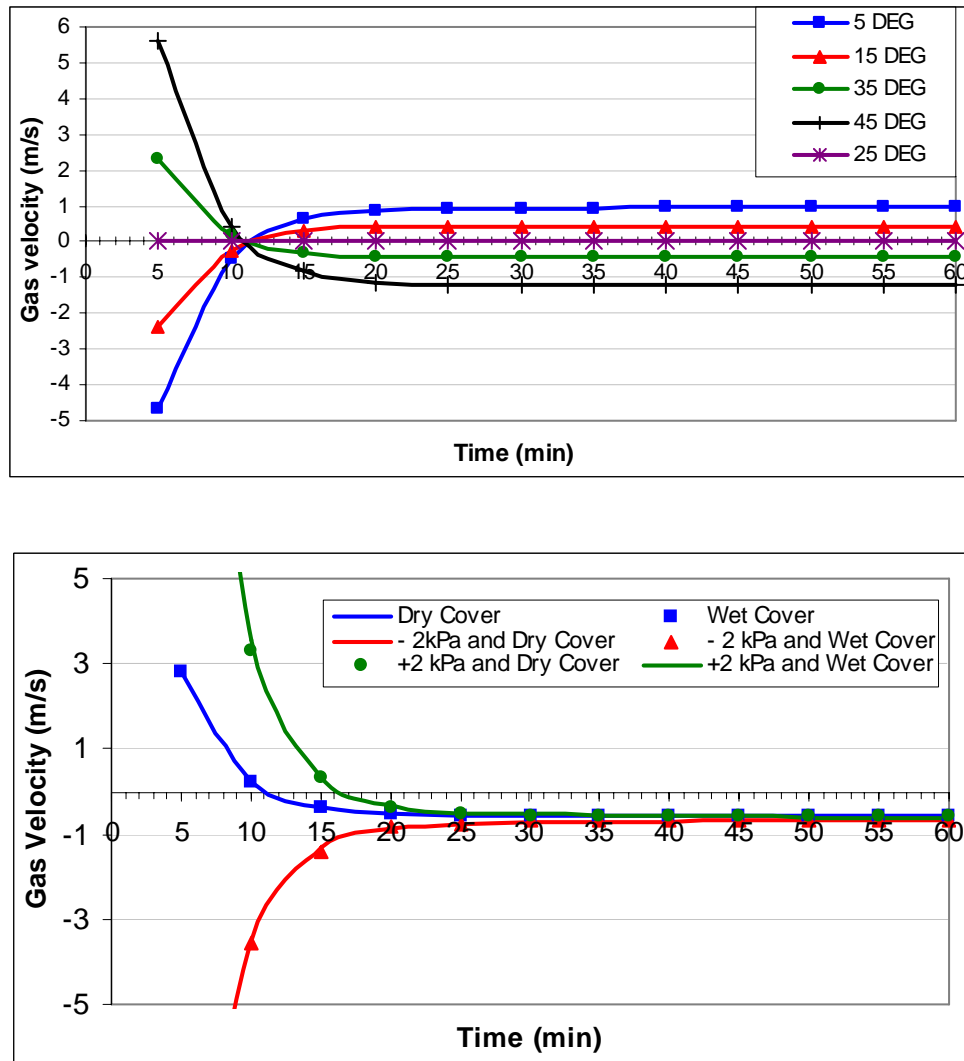


Figure 9. Transient pipe gas velocities for various atmospheric temperatures (top) and pressures at 36 °C (bottom)

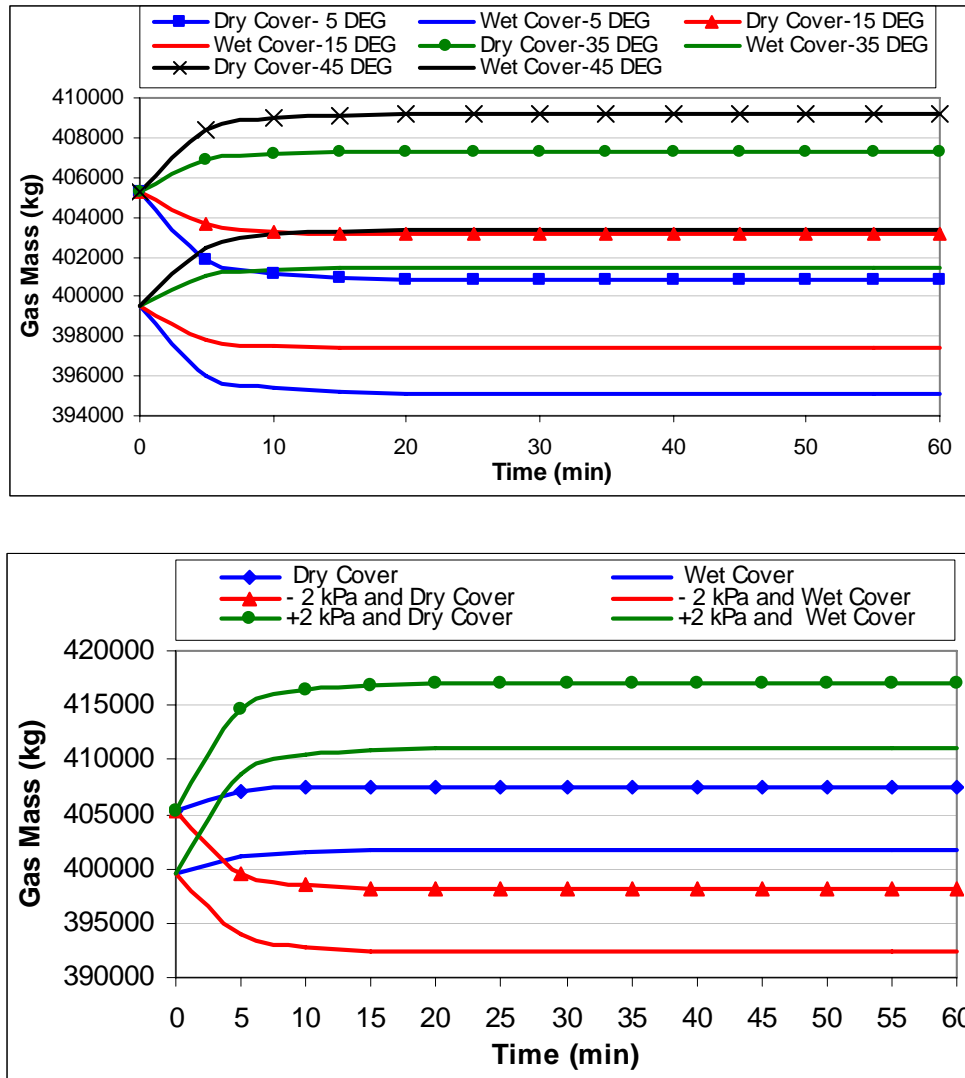


Figure 10. Transient gas mass in the dump for various atmospheric temperatures (top) and pressures at 36 °C (bottom)

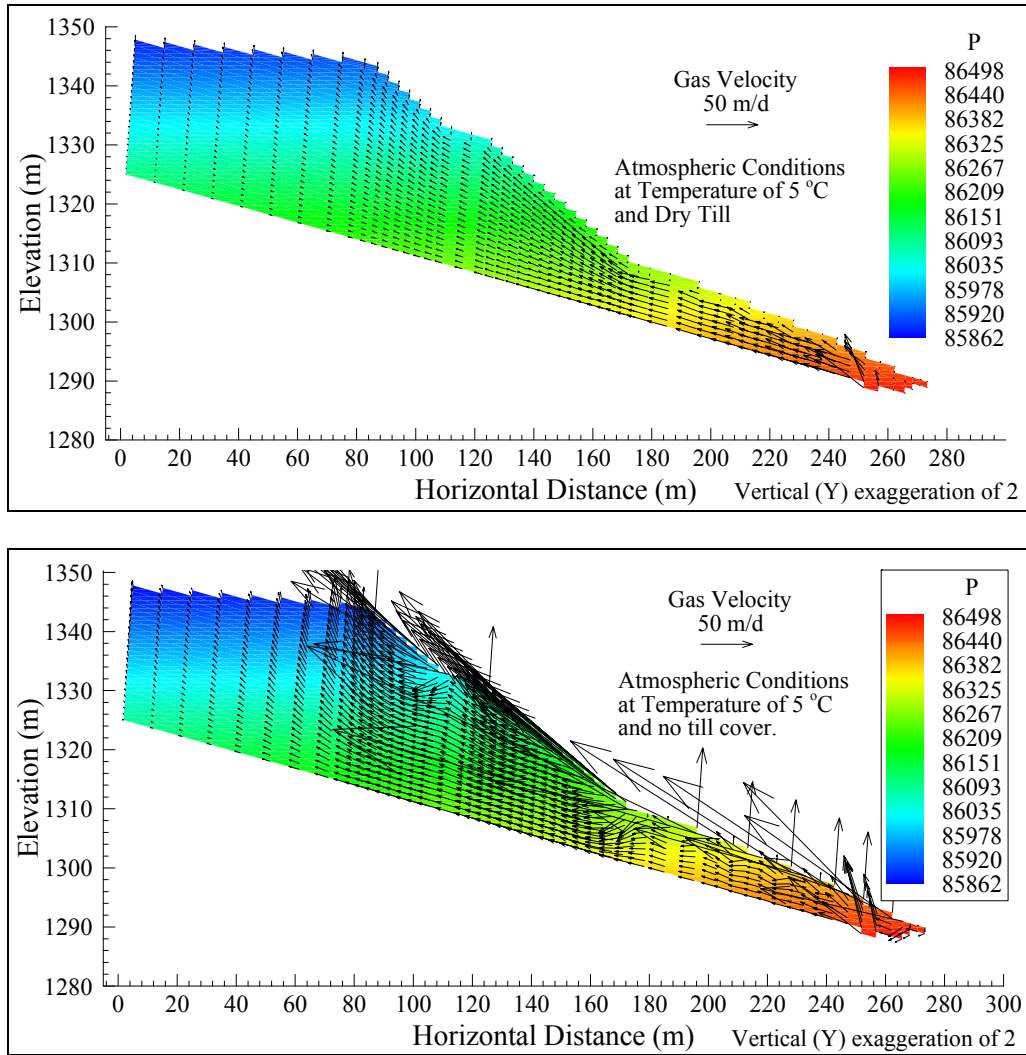


Figure 11. Simulated conditions at 5 °C without a till cover (bottom) compared to conditions with a dry till cover (top)

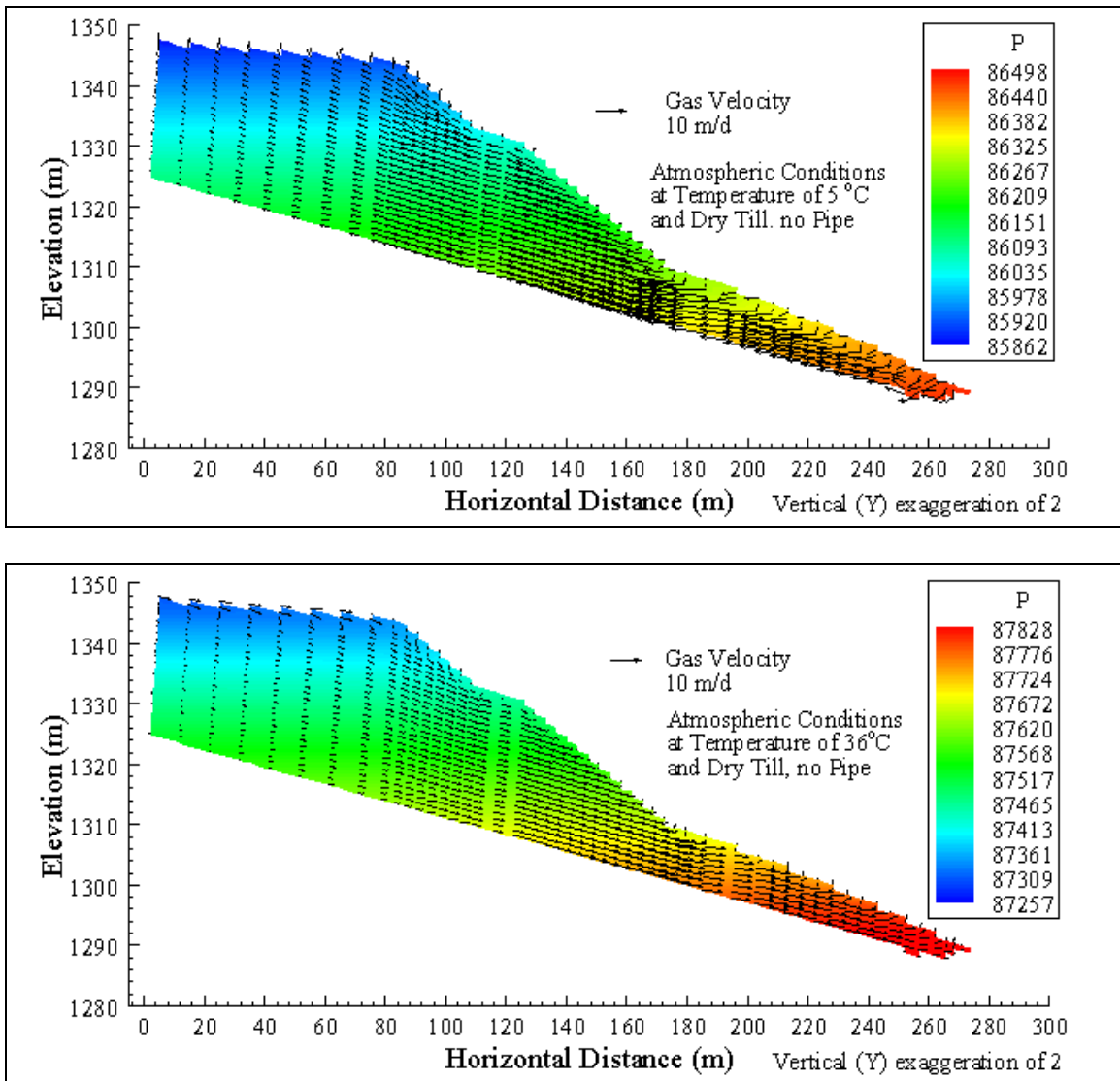


Figure 12. Simulated conditions without a pipe for a dry till cover at 5 °C (top) and 36 °C (bottom)

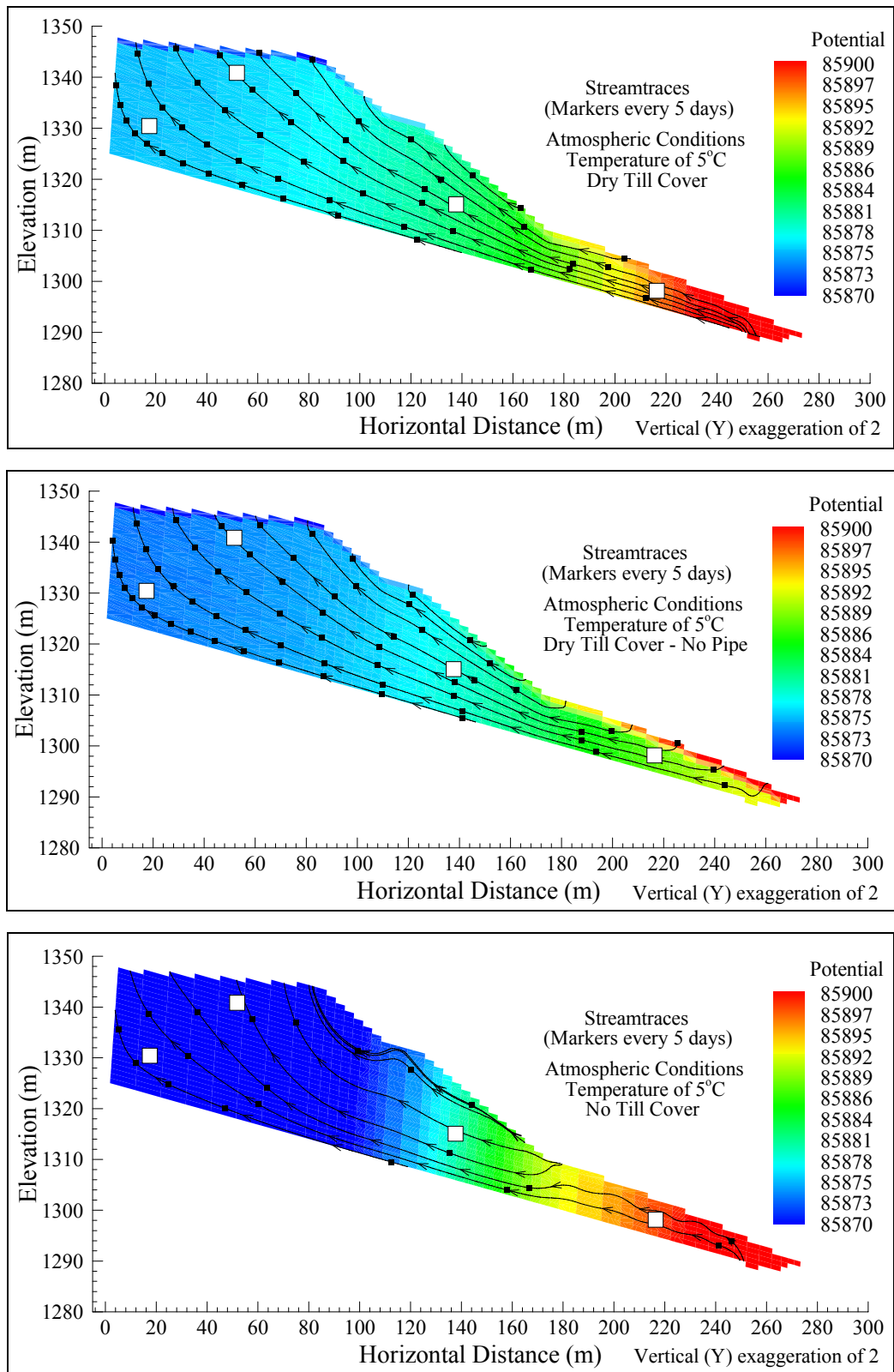


Figure 13. Pneumatic potential and streamtraces at 5 °C for the dry till cover with the pipe (top), without a pipe (middle) and with a pipe but without a till cover (bottom)

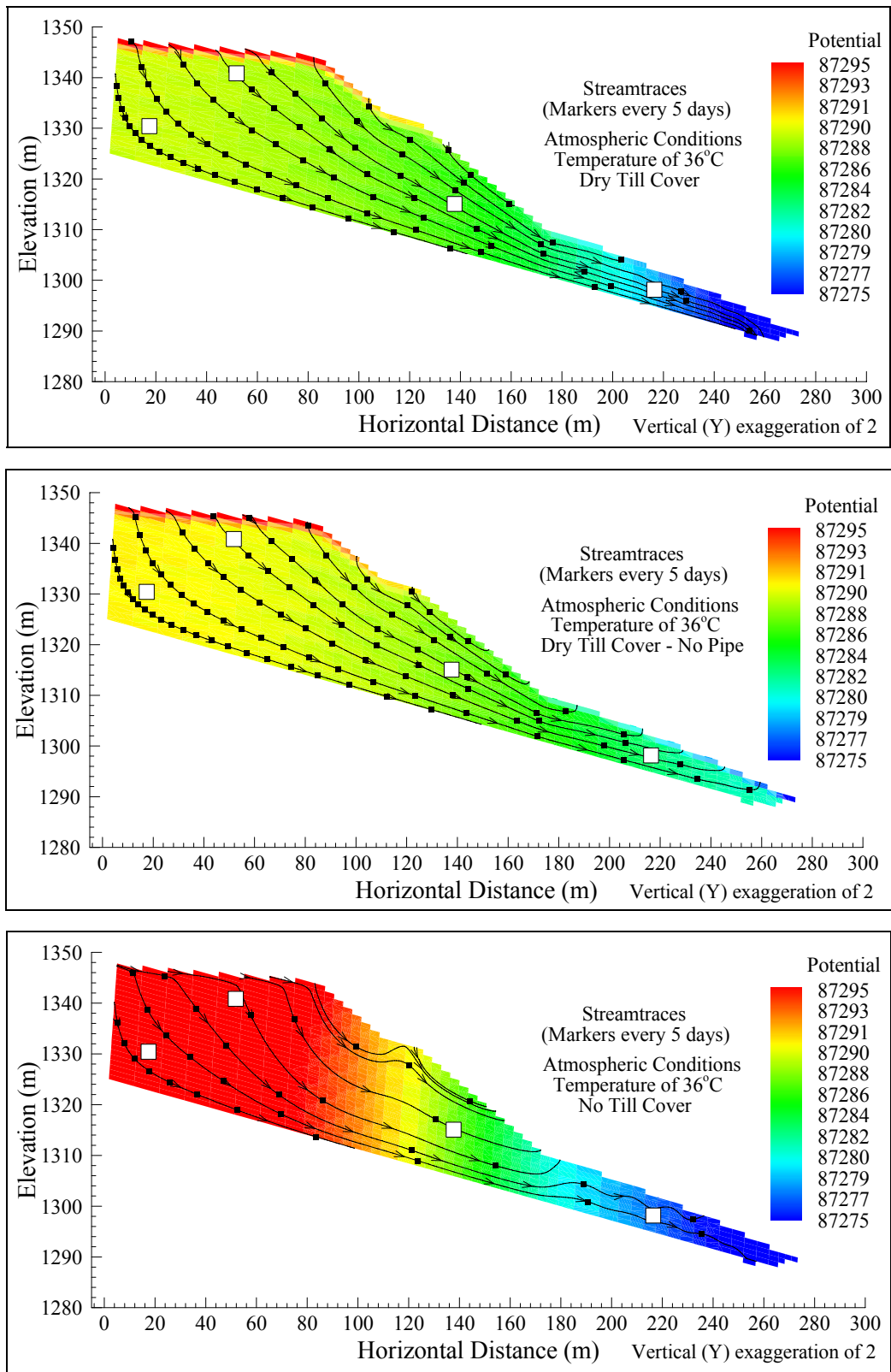


Figure 14. Pneumatic potential and streamtraces at 36 °C for the dry till cover with the pipe (top), without a pipe (middle) and with a pipe but without a till cover (bottom)

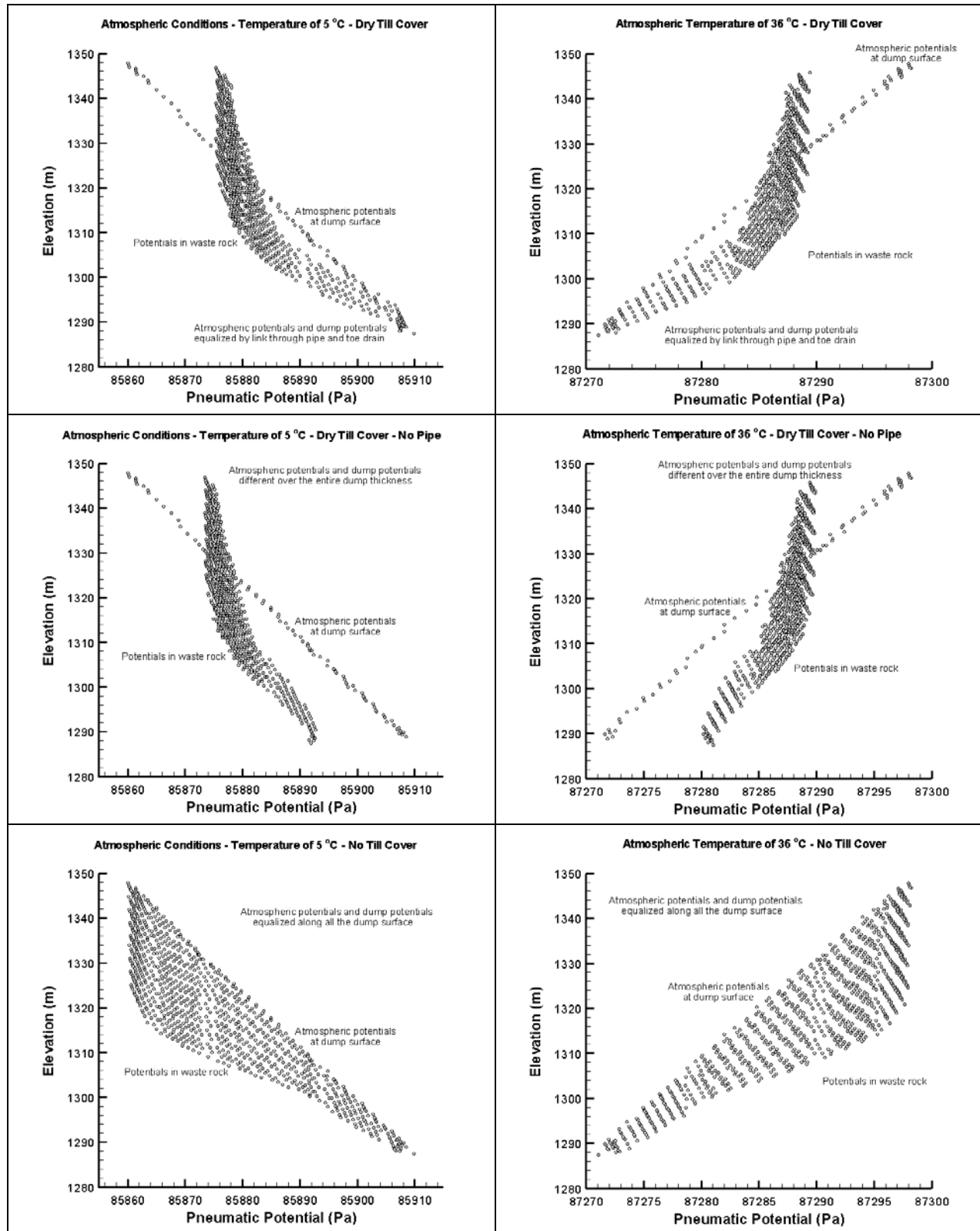


Figure 15. Vertical distribution of pneumatic potentials at 5 °C (left) and 36 °C (right) for the dry till cover with the pipe (top), without a pipe (middle) and without a till cover (bottom)

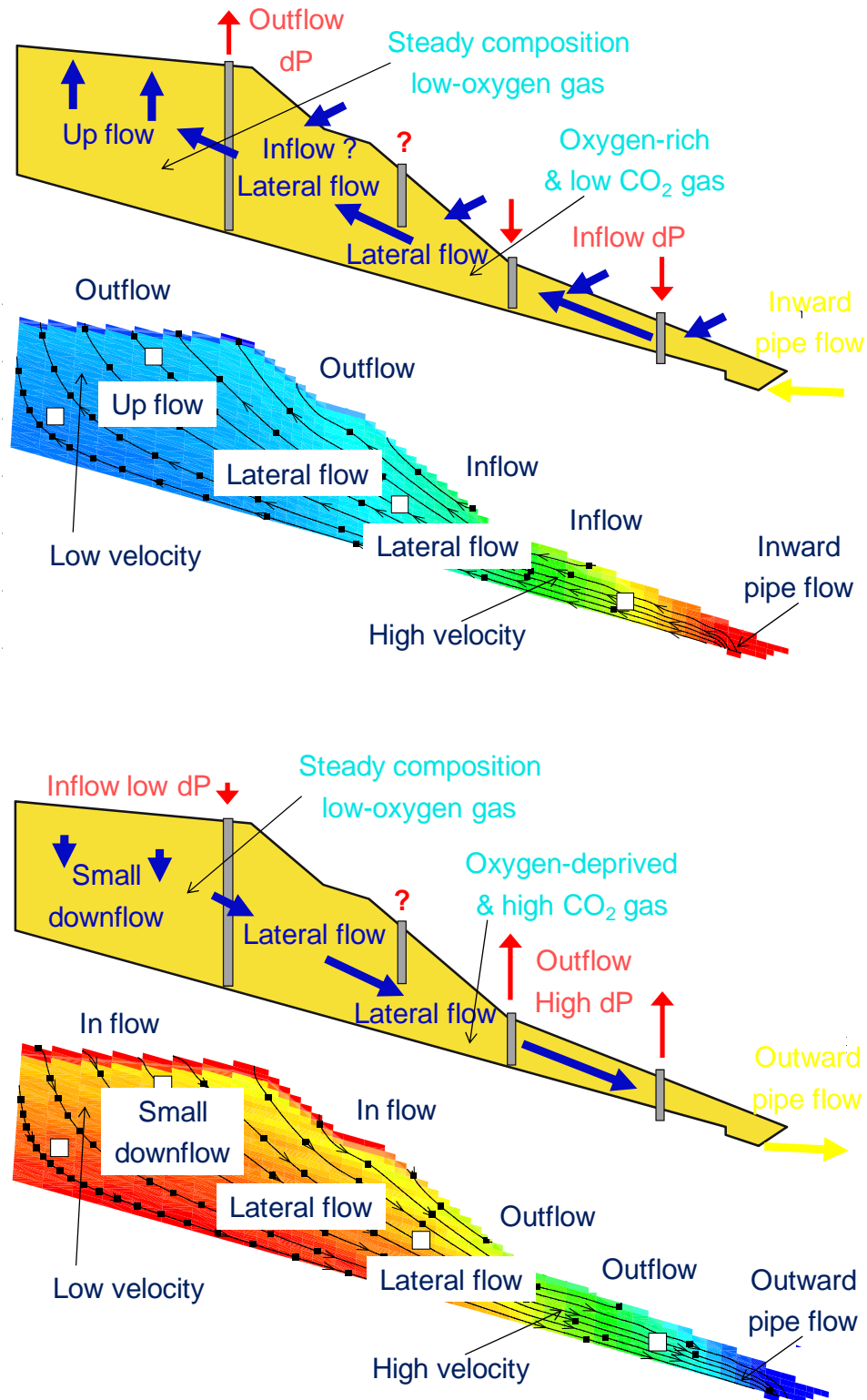


Figure 16. Comparison of the conceptual model of gas flow with numerical results for low (top) and high (bottom) atmospheric temperatures

Appendix

APPENDIX 1:
COMPLEMENTARY SIMULATION RESULTS AND FIGURES

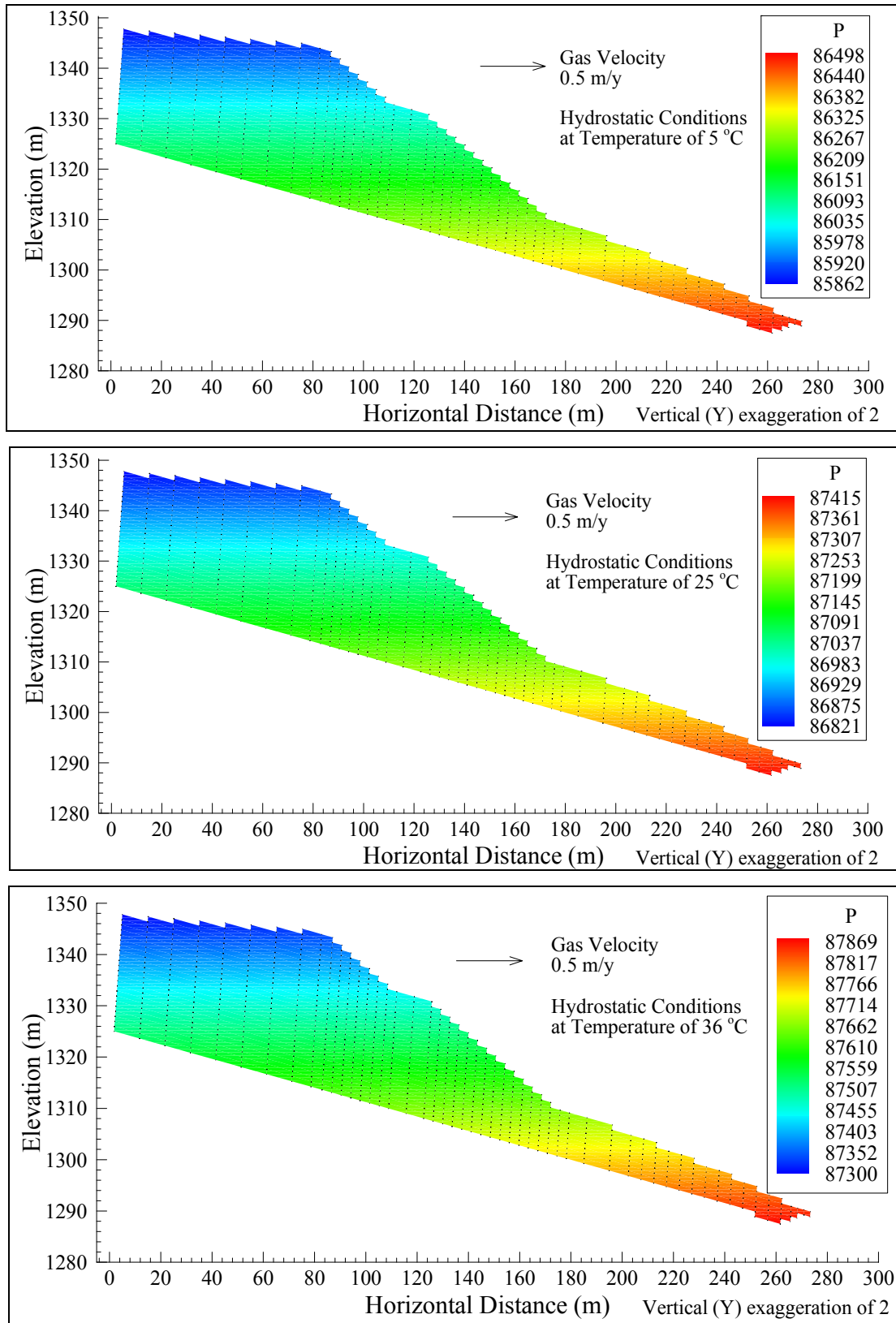


Figure A1.1. Gas pressure distributions under hydrostatic conditions at 5, 25 and 36 °C

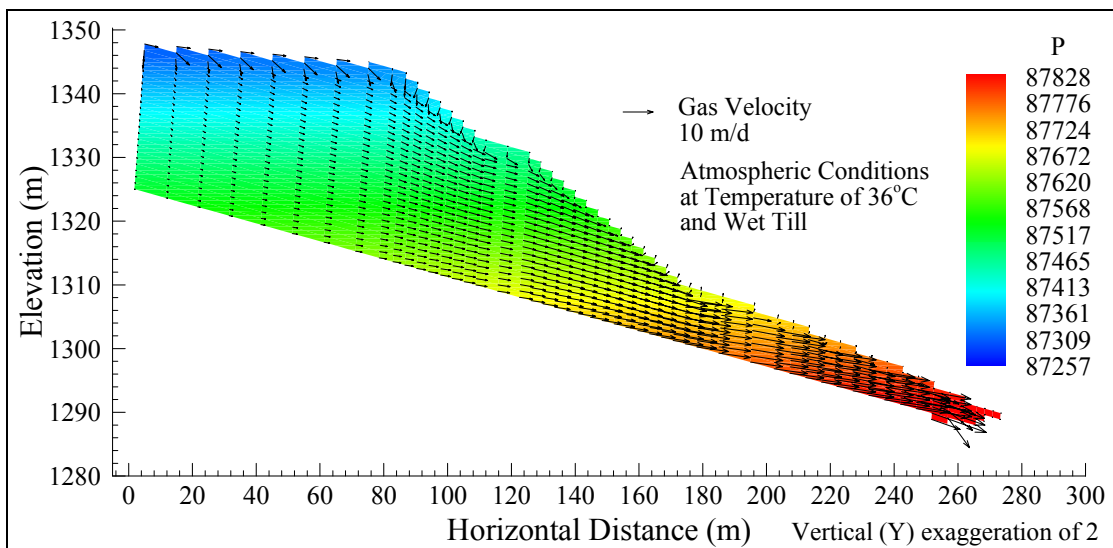
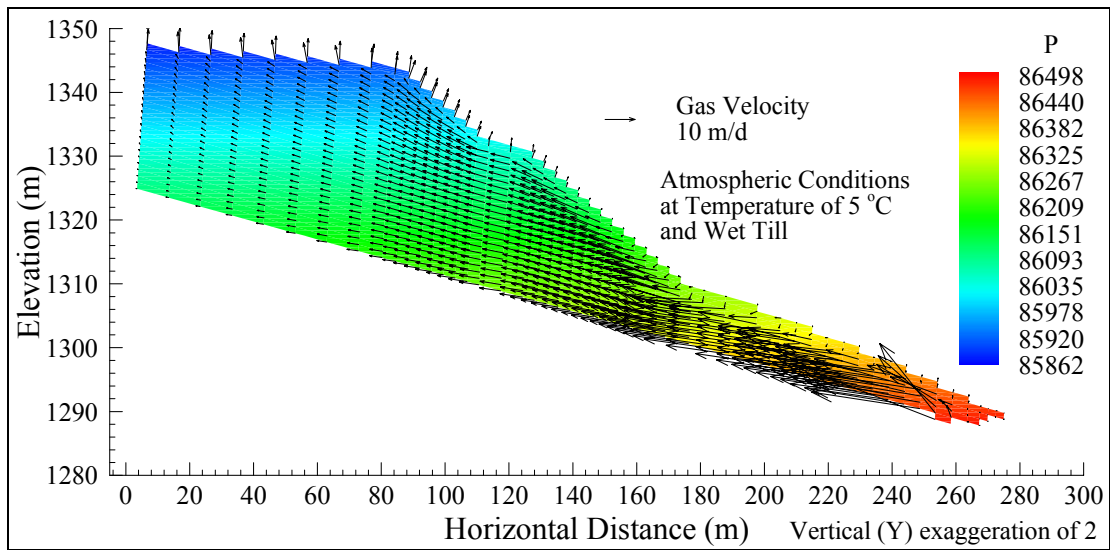


Figure A1.2. Gas pressure and velocity after 12 hours for wet till cover at low atmospheric temperature (5 °C) (top) and high atmospheric temperature (36 °C) (bottom).

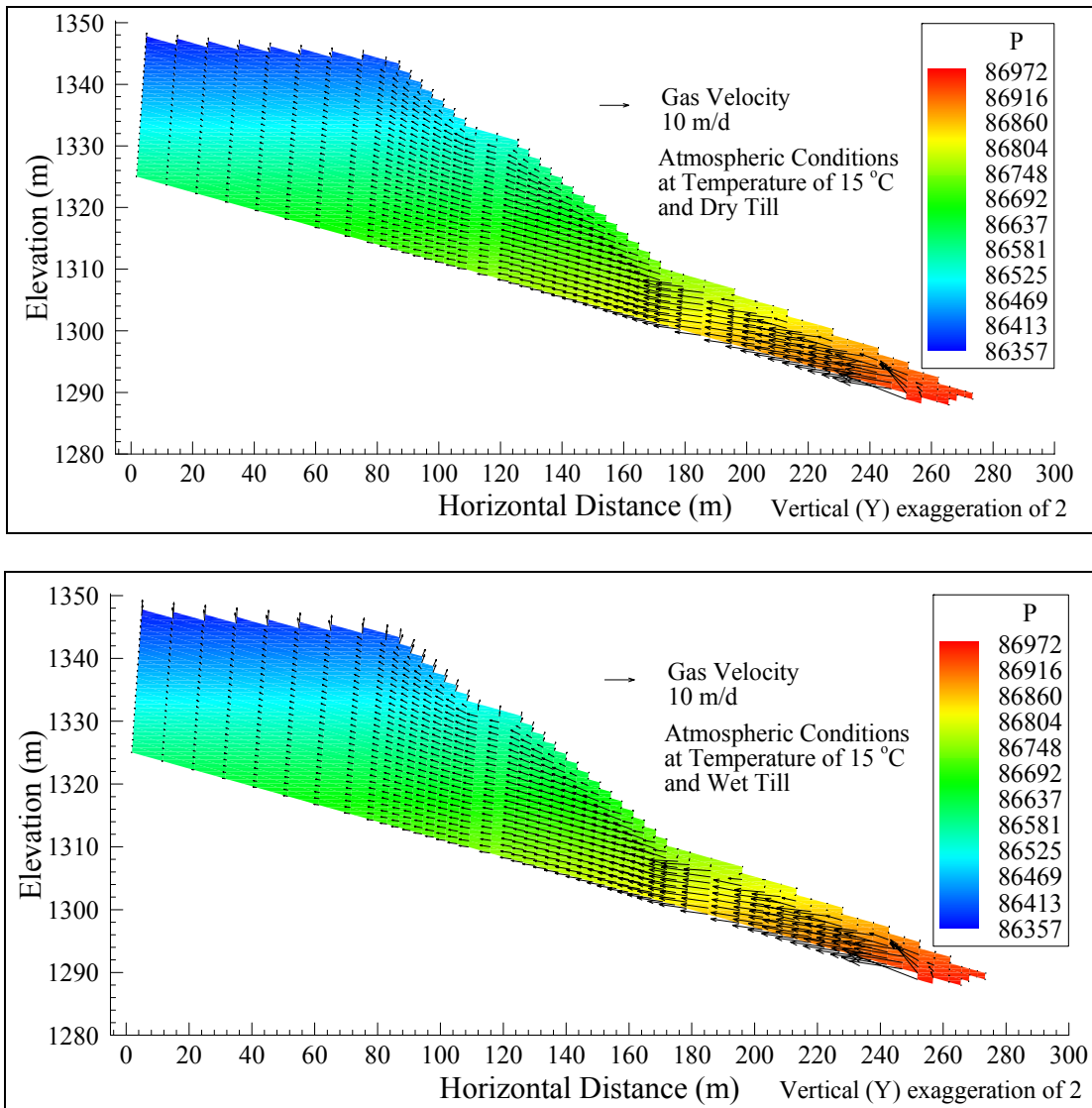


Figure A1.3. Gas pressure and velocity after 12 hours at 15 °C atmospheric temperature for dry (top) and wet (bottom) till cover.

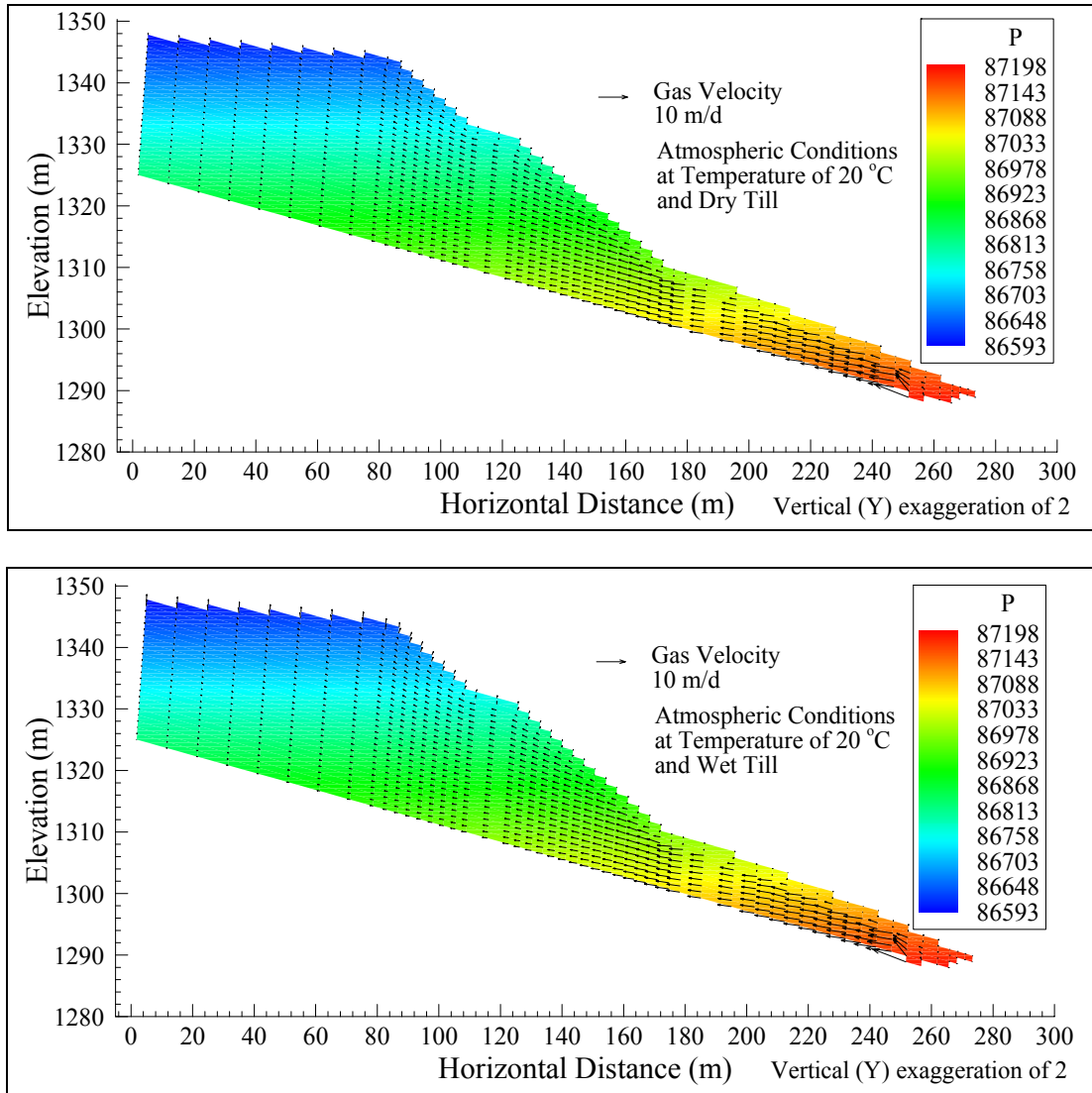


Figure A1.4. Gas pressure and velocity after 12 hours at 20 °C atmospheric temperature for dry (top) and wet (bottom) till cover.

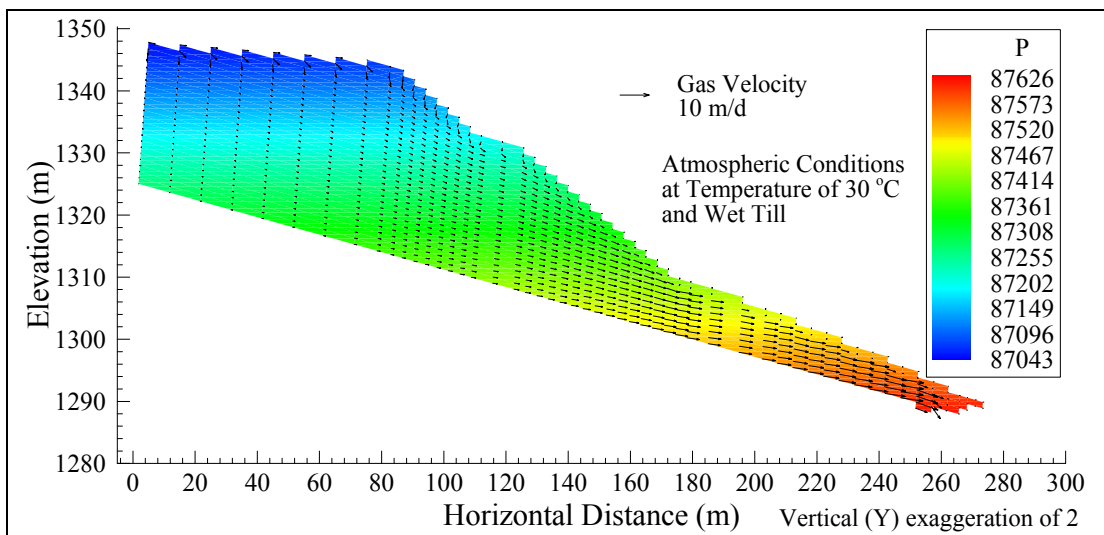
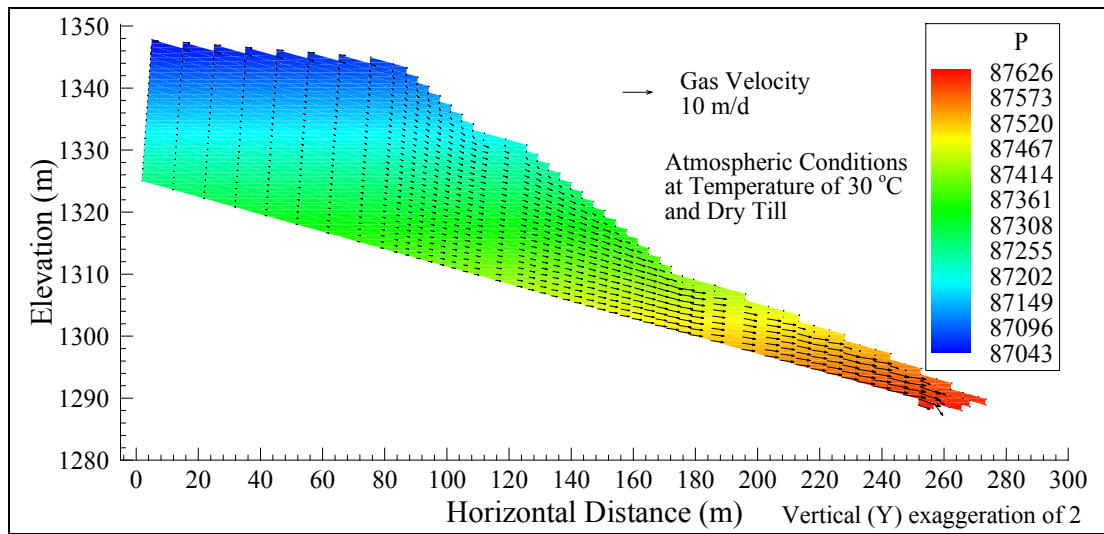


Figure A1.5. Gas pressure and velocity after 12 hours at 30 °C atmospheric temperature for dry (top) and wet (bottom) till cover.

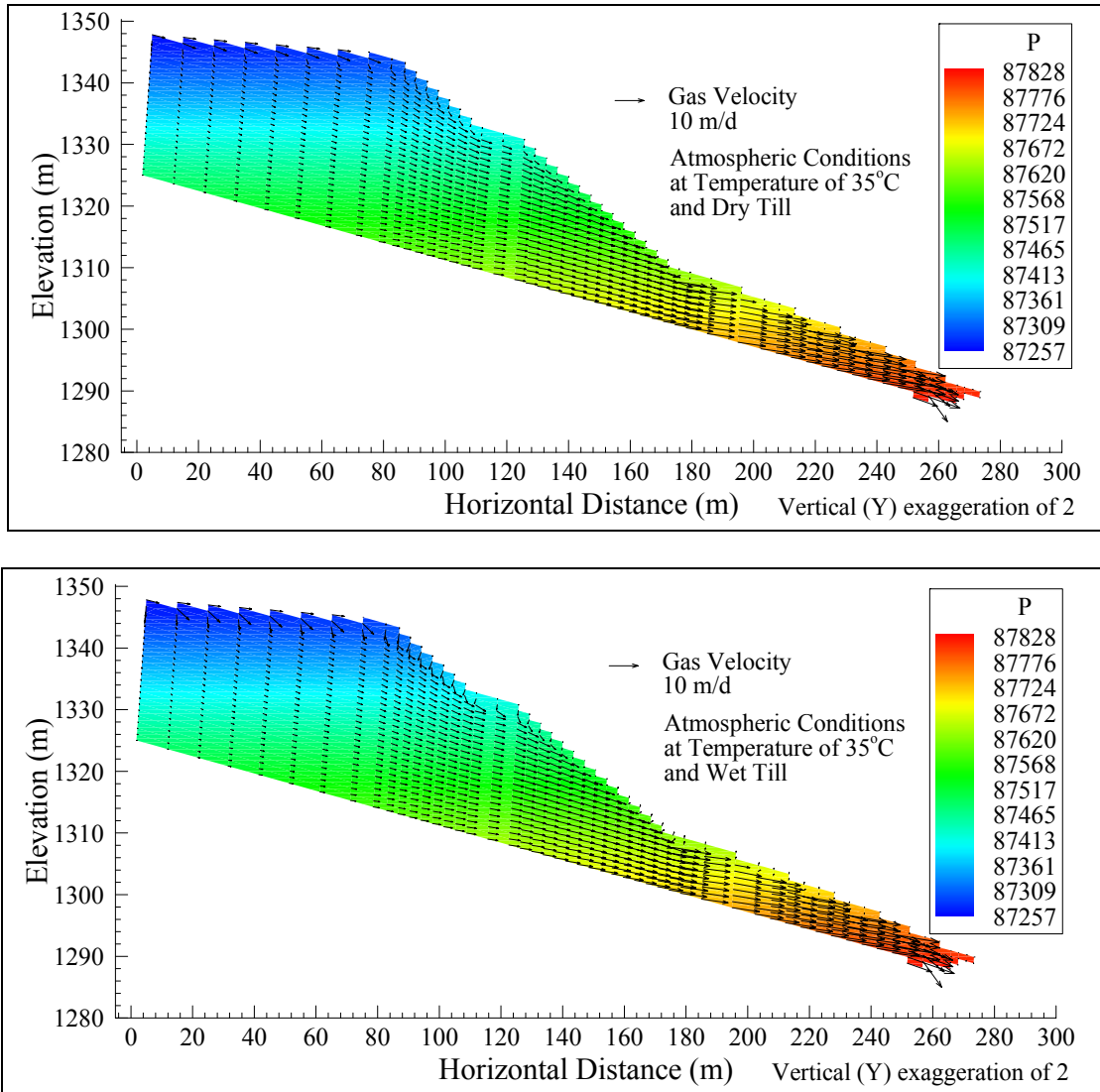


Figure A1.6. Gas pressure and velocity after 12 hours at 35 °C atmospheric temperature for dry (top) and wet (bottom) till cover.

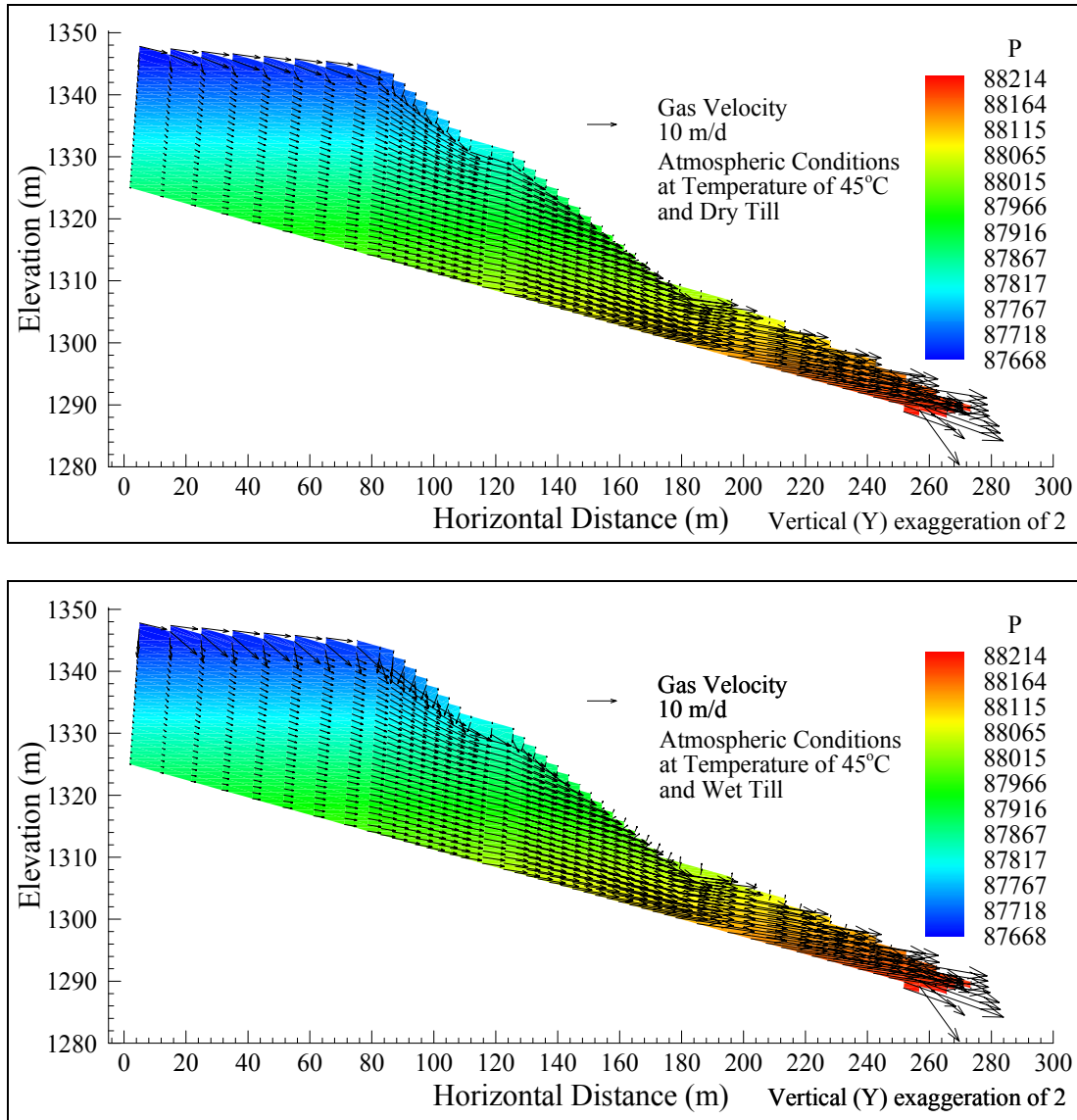


Figure A1.7. Gas pressure and velocity after 12 hours at 45 °C atmospheric temperature for dry (top) and wet (bottom) till cover.

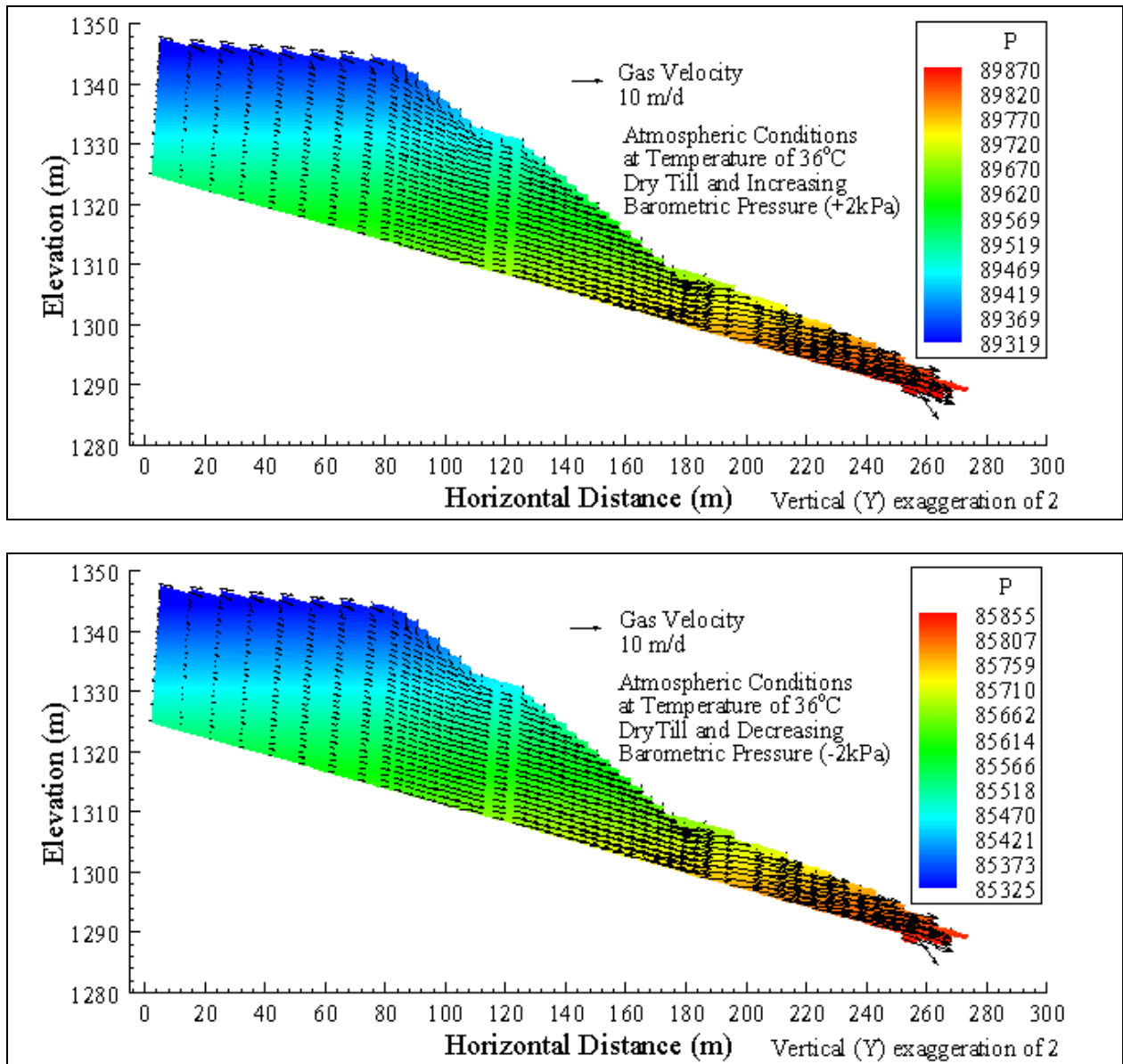


Figure A1.8. Gas pressure and velocity after 12 hours at 36 °C atmospheric temperature for dry till cover at higher (+2 kPa, top) and lower (-2 kPa, bottom) atmospheric pressure.

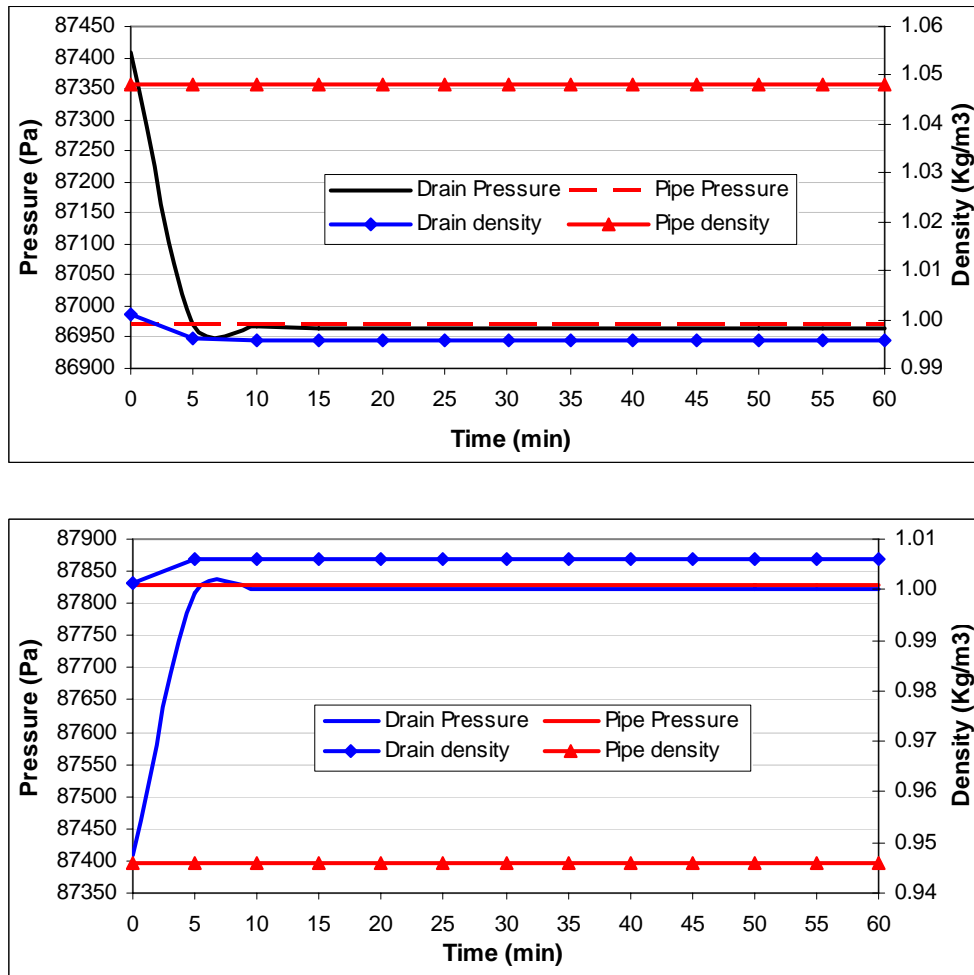


Figure A1.9. Gas pressure and density in the toe drain and pipe versus time at 15 °C (top) and 36 °C (bottom) atmospheric temperature

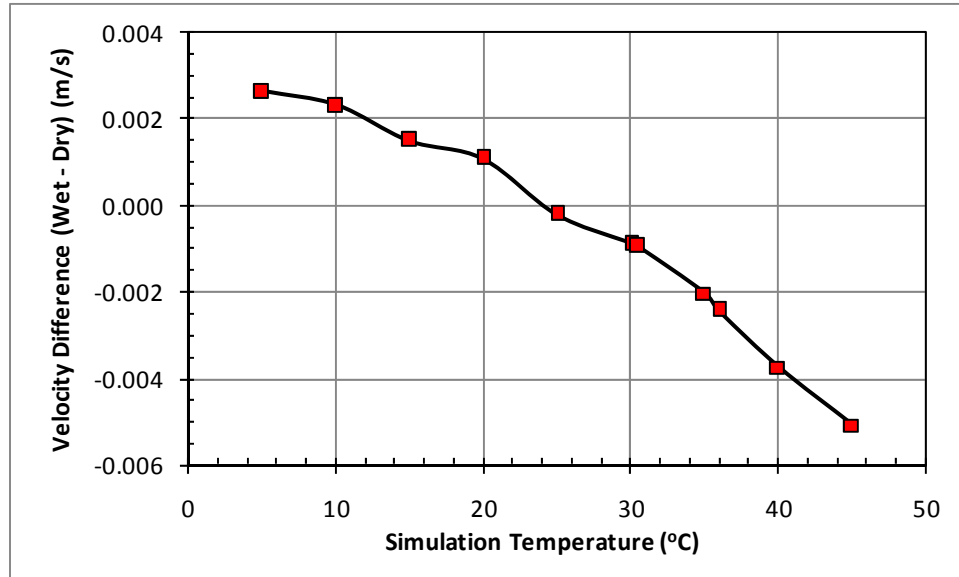


Figure A1.10. Gas velocity difference in the pipe versus temperature in the cases with wet and dry till cover (the difference is the wet till velocity minus the dry till velocity)

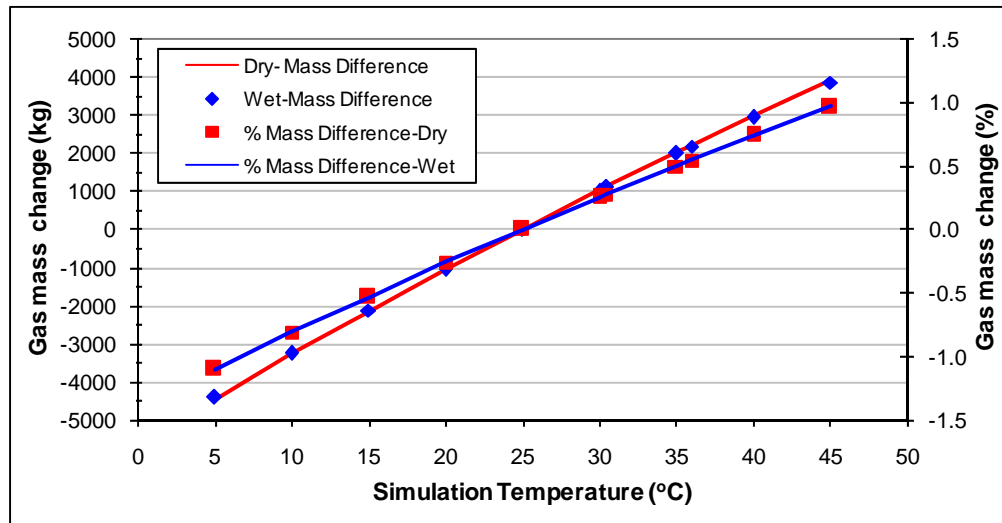


Figure A1.11. Change in gas mass in the dump versus temperature

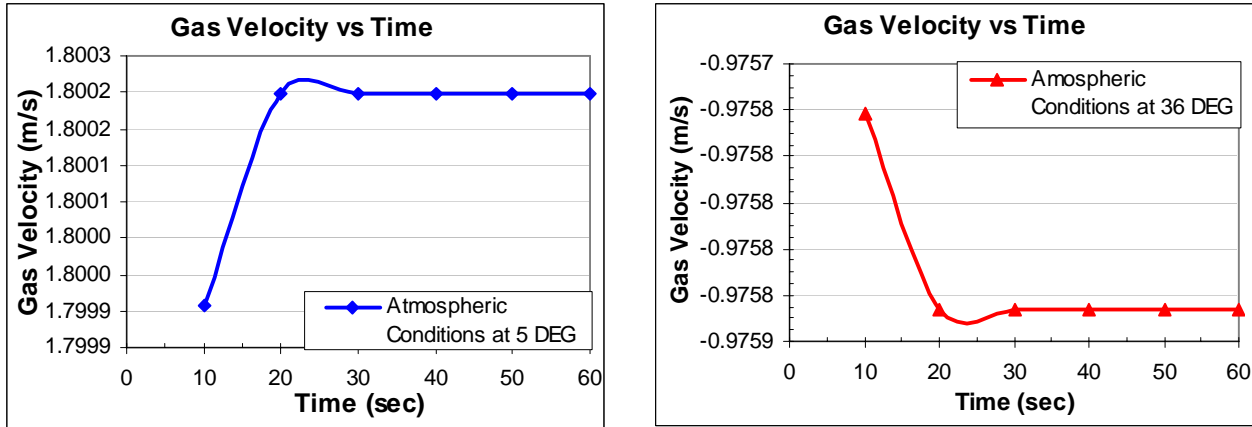


Figure A1.12. Pipe gas velocity versus time without cover at 5 °C (left) and 36 °C (right)

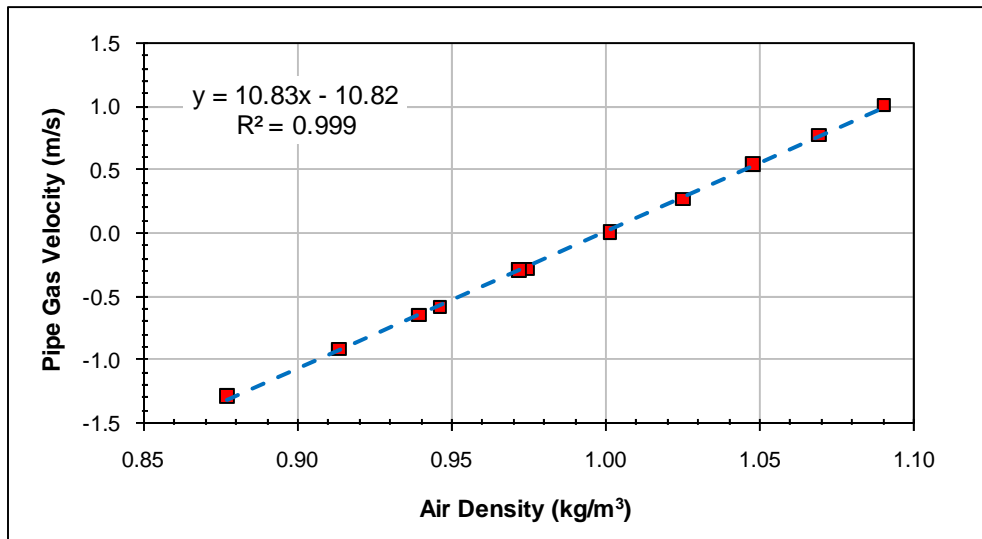


Figure A1.13. Pipe gas velocity versus air density at all simulated atmospheric temperatures

APPENDIX 2:

COMPLITATION OF GAS FLUX, VELOCITY AND MASS

Table A2.1. Gas flux and velocity after 12 h of simulation

Temperature (DEG)	Gas Density (kg/m ³)		Gas Flow (kg/s)		Gas Velocity (m/s)	
	Drain	Pipe	Dry cover	Wet cover	Dry cover	Wet cover
5	1.08982	1.08991	1.39E-01	1.40E-01	1.02E+00	1.02E+00
10	1.06925	1.06934	1.05E-01	1.05E-01	7.79E-01	7.81E-01
15	1.04788	1.04797	7.02E-02	7.04E-02	5.33E-01	5.34E-01
20	1.02533	1.02541	3.54E-02	3.55E-02	2.74E-01	2.75E-01
25	1.00117	1.00125	-9.76E-10	-2.63E-05	-7.76E-09	-2.09E-04
30	0.97494	0.97502	-3.35E-02	-3.36E-02	-2.73E-01	-2.74E-01
30.5	0.97217	0.97225	-3.68E-02	-3.69E-02	-3.01E-01	-3.02E-01
35	0.94606	0.94613	-6.81E-02	-6.83E-02	-5.73E-01	-5.75E-01
36	0.93989	0.93996	-7.52E-02	-7.55E-02	-6.36E-01	-6.39E-01
40	0.91380	0.91387	-1.04E-01	-1.05E-01	-9.08E-01	-9.12E-01
45	0.87746	0.87752	-1.42E-01	-1.43E-01	-1.29E+00	-1.30E+00

Table A2.2. Evolution of the global gas mass in the dump over a 12 h simulation period

Temperature	5 (C)		10 (C)		15 (C)		20 (C)		30 (C)	
	Mass of Gas		Mass of Gas		Mass of Gas		Mass of Gas		Mass of Gas	
Time (h)	Dry Cover	Wet Cover	Dry Cover	Wet Cover	Dry Cover	Wet Cover	Dry Cover	Wet Cover	Dry Cover	Wet Cover
0	4.05E+05	4.00E+05	4.05E+05	4.00E+05	4.05E+05	4.00E+05	4.05E+05	4.00E+05	4.05E+05	4.00E+05
1	4.01E+05	3.95E+05	4.02E+05	3.96E+05	4.03E+05	3.97E+05	4.04E+05	3.98E+05	4.06E+05	4.01E+05
2	4.01E+05	3.95E+05	4.02E+05	3.96E+05	4.03E+05	3.97E+05	4.04E+05	3.98E+05	4.06E+05	4.01E+05
3	4.01E+05	3.95E+05	4.02E+05	3.96E+05	4.03E+05	3.97E+05	4.04E+05	3.98E+05	4.06E+05	4.01E+05
4	4.01E+05	3.95E+05	4.02E+05	3.96E+05	4.03E+05	3.97E+05	4.04E+05	3.98E+05	4.06E+05	4.01E+05
5	4.01E+05	3.95E+05	4.02E+05	3.96E+05	4.03E+05	3.97E+05	4.04E+05	3.98E+05	4.06E+05	4.01E+05
6	4.01E+05	3.95E+05	4.02E+05	3.96E+05	4.03E+05	3.97E+05	4.04E+05	3.98E+05	4.06E+05	4.01E+05
7	4.01E+05	3.95E+05	4.02E+05	3.96E+05	4.03E+05	3.97E+05	4.04E+05	3.98E+05	4.06E+05	4.01E+05
8	4.01E+05	3.95E+05	4.02E+05	3.96E+05	4.03E+05	3.97E+05	4.04E+05	3.98E+05	4.06E+05	4.01E+05
9	4.01E+05	3.95E+05	4.02E+05	3.96E+05	4.03E+05	3.97E+05	4.04E+05	3.98E+05	4.06E+05	4.01E+05
10	4.01E+05	3.95E+05	4.02E+05	3.96E+05	4.03E+05	3.97E+05	4.04E+05	3.98E+05	4.06E+05	4.01E+05
11	4.01E+05	3.95E+05	4.02E+05	3.96E+05	4.03E+05	3.97E+05	4.04E+05	3.98E+05	4.06E+05	4.01E+05
12	4.01E+05	3.95E+05	4.02E+05	3.96E+05	4.03E+05	3.97E+05	4.04E+05	3.98E+05	4.06E+05	4.01E+05
Change (kg)	-4.44E+03	-4.38E+03	-3.28E+03	-3.23E+03	-2.14E+03	-2.12E+03	-1.05E+03	-1.04E+03	1.02E+03	1.01E+03
Change (%)	-1.10	-1.10	-0.81	-0.81	-0.53	-0.53	-0.26	-0.26	0.25	0.25

Temperature	30.5 (C)		35 (C)		36 (C)		40 (C)		45 (C)	
	Mass of Gas		Mass of Gas		Mass of Gas		Mass of Gas		Mass of Gas	
Time (h)	Dry Cover	Wet Cover	Dry Cover	Wet Cover	Dry Cover	Wet Cover	Dry Cover	Wet Cover	Dry Cover	Wet Cover
0	4.05E+05	4.00E+05	4.05E+05	4.00E+05	4.05E+05	4.00E+05	4.05E+05	4.00E+05	4.05E+05	4.00E+05
1	4.06E+05	4.01E+05	4.07E+05	4.01E+05	4.08E+05	4.02E+05	4.08E+05	4.02E+05	4.09E+05	4.03E+05
2	4.06E+05	4.01E+05	4.07E+05	4.01E+05	4.08E+05	4.02E+05	4.08E+05	4.02E+05	4.09E+05	4.03E+05
3	4.06E+05	4.01E+05	4.07E+05	4.01E+05	4.08E+05	4.02E+05	4.08E+05	4.02E+05	4.09E+05	4.03E+05
4	4.06E+05	4.01E+05	4.07E+05	4.01E+05	4.08E+05	4.02E+05	4.08E+05	4.02E+05	4.09E+05	4.03E+05
5	4.06E+05	4.01E+05	4.07E+05	4.01E+05	4.08E+05	4.02E+05	4.08E+05	4.02E+05	4.09E+05	4.03E+05
6	4.06E+05	4.01E+05	4.07E+05	4.01E+05	4.08E+05	4.02E+05	4.08E+05	4.02E+05	4.09E+05	4.03E+05
7	4.06E+05	4.01E+05	4.07E+05	4.01E+05	4.08E+05	4.02E+05	4.08E+05	4.02E+05	4.09E+05	4.03E+05
8	4.06E+05	4.01E+05	4.07E+05	4.01E+05	4.08E+05	4.02E+05	4.08E+05	4.02E+05	4.09E+05	4.03E+05
9	4.06E+05	4.01E+05	4.07E+05	4.01E+05	4.08E+05	4.02E+05	4.08E+05	4.02E+05	4.09E+05	4.03E+05
10	4.06E+05	4.01E+05	4.07E+05	4.01E+05	4.08E+05	4.02E+05	4.08E+05	4.02E+05	4.09E+05	4.03E+05
11	4.06E+05	4.01E+05	4.07E+05	4.01E+05	4.08E+05	4.02E+05	4.08E+05	4.02E+05	4.09E+05	4.03E+05
12	4.06E+05	4.01E+05	4.07E+05	4.01E+05	4.08E+05	4.02E+05	4.08E+05	4.02E+05	4.09E+05	4.03E+05
Change (kg)	1.12E+03	1.10E+03	2.01E+03	1.98E+03	2.21E+03	2.18E+03	2.98E+03	2.93E+03	3.91E+03	3.85E+03
Change (%)	0.28	0.28	0.50	0.50	0.55	0.55	0.74	0.73	0.96	0.96

Table A2.3. Difference between the initial and final gas mass in the dump after 12 hr of simulation

Temperature (DEG)	Mass difference (kg)		Mass Difference (%)	
	Dry Cover	Wet Cover	Dry Cover	Wet Cover
5	-4440	-4380	-1.10	-1.10
10	-3280	-3230	-0.81	-0.81
15	-2140	-2120	-0.53	-0.53
20	-1050	-1040	-0.26	-0.26
25	0	0	0.00	0.00
30	1020	1010	0.25	0.25
30.5	1120	1100	0.28	0.28
35	2010	1980	0.50	0.50
36	2210	2180	0.55	0.55
40	2980	2930	0.74	0.73
45	3910	3850	0.96	0.96

Table A2.4. Gas flux and velocity versus time

Surface (drain-Pipe) 0.1257 (m2) Gas Density 1.08990876 (kg/m3) Atmospheric Temperature 5 (C)					Surface (drain-Pipe) 0.1257 (m2) Gas Density 1.0479672 (kg/m3) Atmospheric Temperature 15 (C)				
Time (min)	Dry Cover		Wet Cover		Time (min)	Dry Cover		Wet Cover	
	Flux (kg/s)	V (m/s)	Flux (kg/s)	V (m/s)		Flux (kg/s)	V (m/s)	Flux (kg/s)	V (m/s)
5	-6.39E-01	-4.66E+00	-6.38E-01	-4.66E+00	5	-3.13E-01	-2.38E+00	-3.32E-01	-2.52E+00
10	-6.90E-02	-5.03E-01	-6.59E-02	-4.81E-01	10	-3.20E-02	-2.43E-01	-3.63E-02	-2.75E-01
15	8.83E-02	6.44E-01	9.01E-02	6.58E-01	15	3.71E-02	2.82E-01	3.62E-02	2.75E-01
20	1.20E-01	8.72E-01	1.21E-01	8.81E-01	20	5.74E-02	4.36E-01	5.75E-02	4.36E-01
25	1.29E-01	9.41E-01	1.30E-01	9.47E-01	25	5.74E-02	4.36E-01	5.75E-02	4.36E-01
30	1.29E-01	9.41E-01	1.30E-01	9.47E-01	30	5.74E-02	4.36E-01	5.75E-02	4.36E-01
35	1.29E-01	9.41E-01	1.30E-01	9.47E-01	35	5.74E-02	4.36E-01	5.75E-02	4.36E-01
40	1.31E-01	9.56E-01	1.32E-01	9.66E-01	40	5.74E-02	4.36E-01	5.75E-02	4.36E-01
45	1.31E-01	9.56E-01	1.32E-01	9.66E-01	45	5.74E-02	4.36E-01	5.75E-02	4.36E-01
50	1.31E-01	9.56E-01	1.32E-01	9.66E-01	50	5.74E-02	4.36E-01	5.75E-02	4.36E-01
55	1.31E-01	9.56E-01	1.32E-01	9.66E-01	55	5.74E-02	4.36E-01	5.75E-02	4.36E-01
60	1.33E-01	9.72E-01	1.34E-01	9.77E-01	60	5.74E-02	4.36E-01	5.75E-02	4.36E-01

Surface (drain-Pipe) 0.1257 (m2) Gas Density 1.08990876 (kg/m3) Atmospheric Temperature 35 (C)					Surface (drain-Pipe) 0.1257 (m2) Gas Density 0.87745614 (kg/m3) Atmospheric temperature 45 (C)				
Time (min)	Dry Cover		Wet Cover		Time (min)	Dry Cover		Wet Cover	
	Flux (kg/s)	V (m/s)	Flux (kg/s)	V (m/s)		Flux (kg/s)	V (m/s)	Flux (kg/s)	V (m/s)
5	3.20E-01	2.33E+00	3.20E-01	2.33E+00	5	6.21E-01	5.63E+00	6.21E-01	5.63E+00
10	2.83E-02	2.07E-01	2.83E-02	2.07E-01	10	4.32E-02	3.92E-01	4.32E-02	3.92E-01
15	-4.09E-02	-2.99E-01	-4.09E-02	-2.99E-01	15	-9.07E-02	-8.22E-01	-9.07E-02	-8.22E-01
20	-5.49E-02	-4.01E-01	-5.50E-02	-4.01E-01	20	-1.27E-01	-1.15E+00	-1.28E-01	-1.16E+00
25	-6.14E-02	-4.48E-01	-6.17E-02	-4.50E-01	25	-1.35E-01	-1.22E+00	-1.36E-01	-1.23E+00
30	-6.14E-02	-4.48E-01	-6.17E-02	-4.50E-01	30	-1.35E-01	-1.22E+00	-1.36E-01	-1.23E+00
35	-6.14E-02	-4.48E-01	-6.17E-02	-4.50E-01	35	-1.35E-01	-1.22E+00	-1.36E-01	-1.23E+00
40	-6.14E-02	-4.48E-01	-6.17E-02	-4.50E-01	40	-1.35E-01	-1.22E+00	-1.36E-01	-1.23E+00
45	-6.14E-02	-4.48E-01	-6.17E-02	-4.50E-01	45	-1.35E-01	-1.22E+00	-1.36E-01	-1.23E+00
50	-6.14E-02	-4.48E-01	-6.17E-02	-4.50E-01	50	-1.35E-01	-1.22E+00	-1.36E-01	-1.23E+00
55	-6.14E-02	-4.48E-01	-6.17E-02	-4.50E-01	55	-1.35E-01	-1.22E+00	-1.36E-01	-1.23E+00
60	-6.14E-02	-4.48E-01	-6.17E-02	-4.50E-01	60	-1.35E-01	-1.22E+00	-1.36E-01	-1.23E+00

Table A2.5. Gas mass in the dump versus time

Time (min)	Temperature = 5 (C)		Temperature = 15 (C)		Temperature = 35 (C)		Temperature = 45 (C)	
	Dry Cover	Wet Cover	Dry Cover	Wet Cover	Dry Cover	Wet Cover	Dry Cover	Wet Cover
0	4.05E+05	4.00E+05	4.05E+05	4.00E+05	4.05E+05	4.00E+05	4.05E+05	4.00E+05
5	4.02E+05	3.96E+05	4.04E+05	3.98E+05	4.07E+05	4.01E+05	4.08E+05	4.03E+05
10	4.01E+05	3.95E+05	4.03E+05	3.98E+05	4.07E+05	4.01E+05	4.09E+05	4.03E+05
15	4.01E+05	3.95E+05	4.03E+05	3.97E+05	4.07E+05	4.01E+05	4.09E+05	4.03E+05
20	4.01E+05	3.95E+05	4.03E+05	3.97E+05	4.07E+05	4.01E+05	4.09E+05	4.03E+05
25	4.01E+05	3.95E+05	4.03E+05	3.97E+05	4.07E+05	4.01E+05	4.09E+05	4.03E+05
30	4.01E+05	3.95E+05	4.03E+05	3.97E+05	4.07E+05	4.01E+05	4.09E+05	4.03E+05
35	4.01E+05	3.95E+05	4.03E+05	3.97E+05	4.07E+05	4.01E+05	4.09E+05	4.03E+05
40	4.01E+05	3.95E+05	4.03E+05	3.97E+05	4.07E+05	4.01E+05	4.09E+05	4.03E+05
45	4.01E+05	3.95E+05	4.03E+05	3.97E+05	4.07E+05	4.01E+05	4.09E+05	4.03E+05
50	4.01E+05	3.95E+05	4.03E+05	3.97E+05	4.07E+05	4.01E+05	4.09E+05	4.03E+05
55	4.01E+05	3.95E+05	4.03E+05	3.97E+05	4.07E+05	4.01E+05	4.09E+05	4.03E+05
60	4.01E+05	3.95E+05	4.03E+05	3.97E+05	4.07E+05	4.01E+05	4.09E+05	4.03E+05
Difference	-4.43E+03	-4.37E+03	-2.13E+03	-2.10E+03	2.01E+03	1.95E+03	3.89E+03	3.83E+03

Table A2.6. Gas pressure and density at the drain-pipe boundary versus time

Atm Temp =5 (C); Ppipe=8.64+04 (Pa); Humid mean molar mass=0.02914						
Time (min)	Pdrain (Pa) at 25 (C)	P pipe (Pa) at 5 (C)	Water vapor fraction (drain)	Humid mean molar mass	Gas density- (kg/m3)-Drain	Air density (kg/m3)-Pipe
0	8.74E+04	8.65E+04	0.036140	0.028394	1.0011703	1.08987654
5	8.65E+04	8.65E+04	0.036520	0.028383	0.9903876	1.08987654
10	8.65E+04	8.65E+04	0.036523	0.028383	0.9902926	1.08987654
15	8.65E+04	8.65E+04	0.036524	0.028383	0.9902689	1.08987654
20	8.65E+04	8.65E+04	0.036524	0.028383	0.9902570	1.08987654
25	8.65E+04	8.65E+04	0.036524	0.028383	0.9902570	1.08987654
30	8.65E+04	8.65E+04	0.036524	0.028383	0.9902570	1.08987654
35	8.65E+04	8.65E+04	0.036524	0.028383	0.9902570	1.08987654
40	8.65E+04	8.65E+04	0.036524	0.028383	0.9902570	1.08987654
45	8.65E+04	8.65E+04	0.036524	0.028383	0.9902570	1.08987654
50	8.65E+04	8.65E+04	0.036524	0.028383	0.9902570	1.08987654
55	8.65E+04	8.65E+04	0.036524	0.028383	0.9902570	1.08987654
60	8.65E+04	8.65E+04	0.036524	0.028383	0.9902570	1.08987654
Atm Temp =15 (C); Ppipe=8.70+04 (Pa); Humid mean molar mass=0.02887						
Time (min)	Pdrain (Pa) at 25 (C)	P pipe (Pa) at 15 (C)	Water vapor fraction (drain)	Humid mean molar mass	Gas density- (kg/m3)-Drain	Air density (kg/m3)-Pipe
0	8.74E+04	8.70E+04	0.036140	0.028394	1.00117032	1.0479672
5	8.70E+04	8.70E+04	0.036322	0.028389	0.99596914	1.0479672
10	8.70E+04	8.70E+04	0.036324	0.028389	0.99592164	1.0479672
15	8.70E+04	8.70E+04	0.036324	0.028389	0.99590977	1.0479672
20	8.70E+04	8.70E+04	0.036325	0.028389	0.99589789	1.0479672
25	8.70E+04	8.70E+04	0.036325	0.028389	0.99589789	1.0479672
30	8.70E+04	8.70E+04	0.036325	0.028389	0.99589789	1.0479672
35	8.70E+04	8.70E+04	0.036325	0.028389	0.99589789	1.0479672
40	8.70E+04	8.70E+04	0.036325	0.028389	0.99589789	1.0479672
45	8.70E+04	8.70E+04	0.036325	0.028389	0.99589789	1.0479672
50	8.70E+04	8.70E+04	0.036325	0.028389	0.99589789	1.0479672
55	8.70E+04	8.70E+04	0.036325	0.028389	0.99589789	1.0479672
60	8.70E+04	8.70E+04	0.036325	0.028389	0.99589789	1.0479672
Atm Temp =35 (C); Ppipe=8.78+04 (Pa); Humid mean molar mass=0.02760						
Time (min)	Pdrain (Pa) at 25 (C)	P pipe (Pa) at 35 (C)	Water vapor fraction (drain)	Humid mean molar mass	Gas densité (kg/m3)Drain	Air densité (kg/m3)-Pipe
0	8.74E+04	8.78E+04	0.036140	0.028394	1.00117032	0.94612856
5	8.78E+04	8.78E+04	0.035972	0.028399	1.00602776	0.94612856
10	8.78E+04	8.78E+04	0.035970	0.028399	1.00607527	0.94612856
15	8.78E+04	8.78E+04	0.035970	0.028399	1.00608714	0.94612856
20	8.78E+04	8.78E+04	0.035970	0.028399	1.00608714	0.94612856
25	8.78E+04	8.78E+04	0.035970	0.028399	1.00608714	0.94612856
30	8.78E+04	8.78E+04	0.035970	0.028399	1.00608714	0.94612856
35	8.78E+04	8.78E+04	0.035970	0.028399	1.00608714	0.94612856
40	8.78E+04	8.78E+04	0.035970	0.028399	1.00608714	0.94612856
45	8.78E+04	8.78E+04	0.035970	0.028399	1.00608714	0.94612856
50	8.78E+04	8.78E+04	0.035970	0.028399	1.00608714	0.94612856
55	8.78E+04	8.78E+04	0.035970	0.028399	1.00608714	0.94612856
60	8.78E+04	8.78E+04	0.035970	0.028399	1.00608714	0.94612856
Atm Temp =45 (C); Ppipe=8.82+04 (Pa); Humid mean molar mass=0.026314						
Time (min)	Pdrain (Pa) at 25 (C)	P pipe (Pa) at 45 (C)	Water vapor fraction (drain)	Humid mean molar mass	Gas density (kg/m3)-Drain	Air density (kg/m3)-Pipe
0	8.74E+04	8.82E+04	0.036140	0.028394	1.00117032	0.87751905
5	8.82E+04	8.82E+04	0.035817	0.028404	1.01055236	0.87751905
10	8.82E+04	8.82E+04	0.035813	0.028404	1.01065924	0.87751905
15	8.82E+04	8.82E+04	0.035812	0.028404	1.01068299	0.87751905
20	8.82E+04	8.82E+04	0.035812	0.028404	1.01068299	0.87751905
25	8.82E+04	8.82E+04	0.035812	0.028404	1.01069487	0.87751905
30	8.82E+04	8.82E+04	0.035812	0.028404	1.01069487	0.87751905
35	8.82E+04	8.82E+04	0.035812	0.028404	1.01069487	0.87751905
40	8.82E+04	8.82E+04	0.035812	0.028404	1.01069487	0.87751905
45	8.82E+04	8.82E+04	0.035812	0.028404	1.01069487	0.87751905
50	8.82E+04	8.82E+04	0.035812	0.028404	1.01069487	0.87751905
55	8.82E+04	8.82E+04	0.035812	0.028404	1.01069487	0.87751905
60	8.82E+04	8.82E+04	0.035812	0.028404	1.01069487	0.87751905

Table A2.7. Gas mass and velocity at the pipe at 36 °C atmospheric temperature and normal atmospheric pressure

Normal Pressure at Atmospheric Temperature of 36 °C						
Surface (Drain-Pipe)	0.1257	(m ²)				
Atmospheric Temperature	36	(C)				
Gas Density	0.93988531	(kg/m ³)				
Time (min)	Dry Cover			Wet Cover		
	Gas mass (kg)	Gas Flow (kg/s)	Gas Velocity (m/s)	Gas Mass (kg)	Gas Flow (kg/s)	Gas Velocity (m/s)
0	4.05E+05			4.00E+05		
5	4.07E+05	3.31E-01	2.80E+00	4.01E+05	3.31E-01	2.80E+00
10	4.07E+05	2.57E-02	2.18E-01	4.02E+05	2.57E-02	2.18E-01
15	4.07E+05	-4.70E-02	-3.98E-01	4.02E+05	-4.70E-02	-3.98E-01
20	4.08E+05	-6.26E-02	-5.30E-01	4.02E+05	-6.27E-02	-5.31E-01
25	4.08E+05	-6.89E-02	-5.83E-01	4.02E+05	-6.92E-02	-5.85E-01
30	4.08E+05	-6.89E-02	-5.83E-01	4.02E+05	-6.92E-02	-5.85E-01
35	4.08E+05	-6.89E-02	-5.83E-01	4.02E+05	-6.92E-02	-5.85E-01
40	4.08E+05	-6.89E-02	-5.83E-01	4.02E+05	-6.92E-02	-5.85E-01
45	4.08E+05	-6.89E-02	-5.83E-01	4.02E+05	-6.92E-02	-5.85E-01
50	4.08E+05	-6.89E-02	-5.83E-01	4.02E+05	-6.92E-02	-5.85E-01
55	4.08E+05	-6.89E-02	-5.83E-01	4.02E+05	-6.92E-02	-5.85E-01
60	4.08E+05	-6.89E-02	-5.83E-01	4.02E+05	-6.92E-02	-5.85E-01
Difference (kg)	2210			2170		
Difference (%)	0.5452751			0.54317897		

Table A2.8. Steady state gas mass in the dump at different barometric pressures

Time (h)	Gas Mass (kg)					
	Normal Pressure		Increased Pressure (+2kPa)		Decreased Pressure (-2 kPa)	
	Wet Cover	Dry Cover	Wet Cover	Dry Cover	Wet Cover	Dry Cover
t (0)	4.00E+05	4.05E+05	4.00E+05	4.05E+05	4.00E+05	4.05E+05
t (12h)	4.02E+05	4.08E+05	4.11E+05	4.17E+05	3.92E+05	3.98E+05
Mass (t12h-t0)	2.18E+03	2.21E+03	1.15E+04	1.17E+04	-7.15E+03	-7.25E+03

Table A2.9. Gas mass and velocity at the pipe at 36 °C atmospheric temperature and high (+ 2 kPa) atmospheric pressure

High Barometric Pressure						
Surface (Drain-Pipe)	0.1257		(m ²)			
Atmospheric Temperature	36		(C)			
Gas Density	0.96143124		(kg/m ³)			
Time (min)	Dry Cover			Wet Cover		
	Gas mass (kg)	Gas Flow (kg/s)	Gas Velocity (m/s)	Gas Mass (kg)	Gas flow (kg/s)	Gas Velocity (m/s)
0	4.05E+05			4.00E+05		
5	4.15E+05	1.99E+00	1.65E+01	4.09E+05	2.02E+00	1.67E+01
10	4.16E+05	4.01E-01	3.32E+00	4.10E+05	4.33E-01	3.58E+00
15	4.17E+05	3.92E-02	3.24E-01	4.11E+05	3.91E-02	3.24E-01
20	4.17E+05	-4.26E-02	-3.52E-01	4.11E+05	-4.16E-02	-3.44E-01
25	4.17E+05	-6.35E-02	-5.25E-01	4.11E+05	-6.11E-02	-5.06E-01
30	4.17E+05	-7.02E-02	-5.81E-01	4.11E+05	-6.11E-02	-5.06E-01
35	4.17E+05	-7.02E-02	-5.81E-01	4.11E+05	-6.93E-02	-5.73E-01
40	4.17E+05	-7.02E-02	-5.81E-01	4.11E+05	-6.93E-02	-5.73E-01
45	4.17E+05	-7.02E-02	-5.81E-01	4.11E+05	-6.93E-02	-5.73E-01
50	4.17E+05	-7.02E-02	-5.81E-01	4.11E+05	-7.51E-02	-6.21E-01
55	4.17E+05	-7.02E-02	-5.81E-01	4.11E+05	-7.51E-02	-6.21E-01
60	4.17E+05	-7.02E-02	-5.81E-01	4.11E+05	-7.51E-02	-6.21E-01
Difference (kg)	11680			11510		
Difference (%)	2.88E+00			2.88E+00		

Table A2.10. Gas mass and velocity at the pipe at 36 °C atmospheric temperature and low (- 2 kPa) atmospheric pressure

Low Barometric Pressure						
Surface (Drain-Pipe)	0.1257	(m ²)				
Atmospheric Temperature	36	(C)				
Gas Density	0.91835902	(kg/m ³)				
Time (min)	Dry cover			Wet cover		
	Gas mass (kg)	Gas Flow (kg/s)	Gas Velocity (m/s)	Gas Mass (kg)	Gas Flow (kg/s)	Gas Velocity (m/s)
0	4.05E+05			4.00E+05		
5	4.00E+05	-1.34E+00	-1.16E+01	3.94E+05	-1.32E+00	-1.14E+01
10	3.98E+05	-4.04E-01	-3.50E+00	3.93E+05	-4.13E-01	-3.58E+00
15	3.98E+05	-1.54E-01	-1.33E+00	3.92E+05	-1.65E-01	-1.43E+00
20	3.98E+05	-9.87E-02	-8.55E-01	3.92E+05	-9.74E-02	-8.44E-01
25	3.98E+05	-9.15E-02	-7.92E-01	3.92E+05	-8.78E-02	-7.61E-01
30	3.98E+05	-8.31E-02	-7.20E-01	3.92E+05	-8.03E-02	-6.96E-01
35	3.98E+05	-8.31E-02	-7.20E-01	3.92E+05	-8.03E-02	-6.96E-01
40	3.98E+05	-8.31E-02	-7.20E-01	3.92E+05	-8.03E-02	-6.96E-01
45	3.98E+05	-7.65E-02	-6.63E-01	3.92E+05	-8.03E-02	-6.96E-01
50	3.98E+05	-7.65E-02	-6.63E-01	3.92E+05	-8.03E-02	-6.96E-01
55	3.98E+05	-7.65E-02	-6.63E-01	3.92E+05	-7.81E-02	-6.77E-01
60	3.98E+05	-7.65E-02	-6.63E-01	3.92E+05	-7.81E-02	-6.77E-01
Difference (kg)	-7.25E+03			-7140		
Difference (%)	-1.79E+00			-1.78723404		

Table A2.10. Gas mass in the dump after 12 hr for atmospheric temperatures of 5 and 36 °C with and without a pipe linked to the atmosphere

With Pipe	Gas Mass (kg)			
Time	5°C		36°C	
(h)	Dry Till	Wet Till	Dry Till	Wet Till
t=0	4.05E+05	4.00E+05	4.05E+05	4.00E+05
t= 12h	4.01E+05	3.95E+05	4.08E+05	4.02E+05
(t =12h)-(t =0)	-4.44E+03	-4.38E+03	2.21E+03	2.18E+03
Without Pipe	Gas Mass (kg)			
Time	5°C		36°C	
(h)	Dry Till	Wet Till	Dry Till	Wet Till
t =0	4.05E+05	4.00E+05	4.05E+05	4.00E+05
t = 12h	4.01E+05	3.95E+05	4.08E+05	4.02E+05
(t =12h)-(t =0)	-4.46E+03	-4.40E+03	2.22E+03	2.19E+03
(With Pipe) - (Without Pipe)	20	20	-10	-10

APPENDIX 3:

ESTIMATION OF MATERIAL PROPERTIES

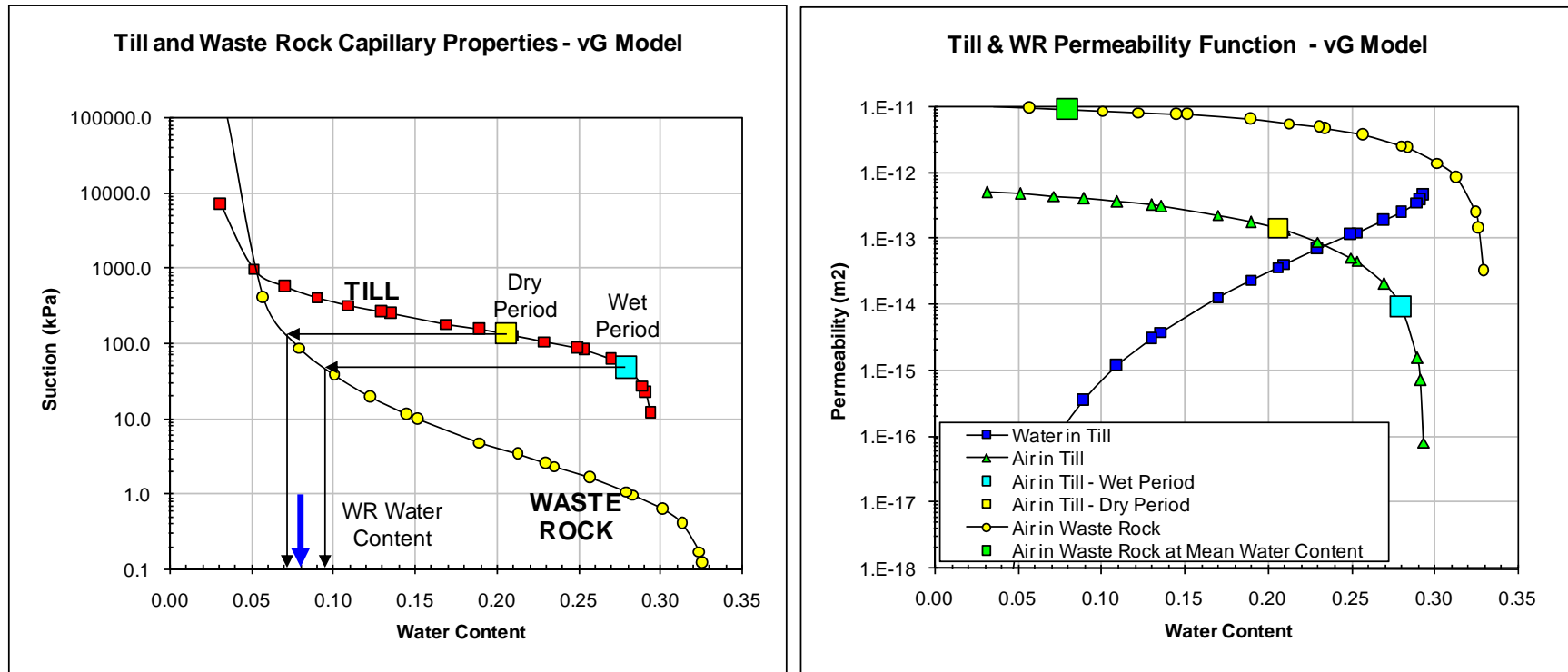


Figure A3.1. Estimated water retention curves (left) and effective permeabilities (right) for the till and waste rock

Table A3.1. Estimated representative water contents and effective air permeabilities of the till cover

Assumed average porosity (saturated water content):	0.295
m	0.55
n	2.22
Residual water saturation Swr	0.10
Permeability (m2)	5.10E-13

DRY CONDITIONS

Range (cm)	Thickness (m)	Water Content	Water Saturation	Effective Sw	kr air	ke air (m2)
0 to 15	0.15	0.10	0.339	0.266	0.772	3.94E-13
15 to 25	0.10	0.14	0.475	0.417	0.595	3.03E-13
25 to 50	0.25	0.20	0.679	0.643	0.311	1.59E-13
50 to 110	0.60	0.22	0.746	0.718	0.222	1.13E-13
110 to 125	0.15	0.20	0.679	0.643	0.311	1.59E-13
Equivalent Vertical ke (m2) (geometric mean):						1.46E-13
Saturation conditions leading to equivalent vertical ke (m2)						
		0.206	0.699	0.665	0.284	1.45E-13

WET CONDITIONS

Range (cm)	Thickness (m)	Water Content	Water Saturation	Effective Sw	kr air	ke air (m2)
0 to 50	0.5	0.28	0.950	0.944	0.018	9.41E-15
50 to 110	0.60	0.26	0.882	0.869	0.070	3.58E-14
110 to 125	0.15	0.24	0.814	0.794	0.140	7.14E-14
Equivalent Vertical ke (m2) (geometric mean):						1.74E-14
Saturation conditions leading to equivalent vertical ke (m2)						
		0.273	0.926	0.918	0.034	1.73E-14

HIGHLY WET CONDITIONS (Supposed high and uniform) (Would be representative of May 2006)

Range (cm)	Thickness (m)	Water Content	Water Saturation	Effective Sw	kr air	ke air (m2)
0 to 125	1.25	0.28	0.950	0.944	0.018	9.41E-15

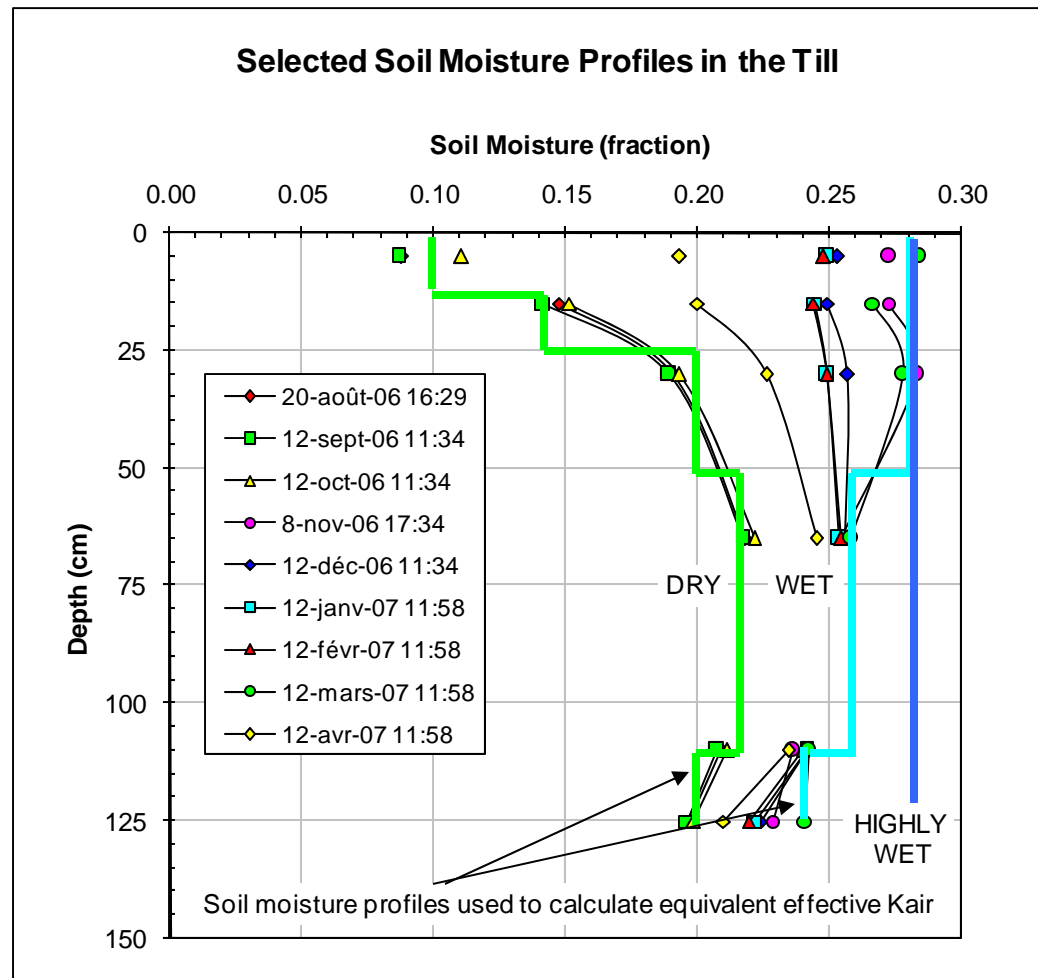


Figure A3.2. Soil moisture profiles used to estimate the equivalent water content and effective air permeability of the till cover